Supporting Information

Controlling Molecularity and Stability of Hydrogen Bonded G-Quadruplexes by Modulating the Structure's Periphery

*Keith B. Sutyak, Peter Y. Zavalij, Michael P. Robinson and Jeffery T. Davis**

Department of Chemistry and Biochemistry, University of Maryland,

College Park, MD. 20742 USA E-Mail: jdavis@umd.edu

Table of Contents

Experimental Procedures

Synthesis of compounds G1-G4

Synthesis of 5′-Benzoyl-2′,3′-Isopropylidene Guanosine (G1)

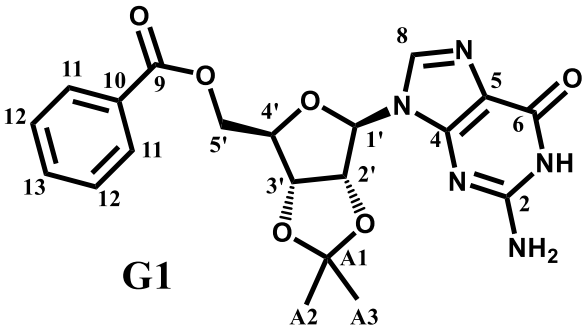

To a suspension of 2′,3′-isopropylidene guanosine (1.00 g, 3.1 mmol), DMAP (20 mg), and triethylamine (0.86 mL, 6.2 mmol) in CH_3CN (38 mL) was added benzoyl chloride (0.53 mL, 4.6 mmol). The mixture was stirred for 16 h, after which tlc analysis (9:1 CH_2Cl_2:MeOH) indicated that the reaction was complete. The reaction mixture was concentrated *in vacuo* to give a white solid. The resulting solid was triturated with MeOH, filtered and vacuum dried to give **G1** as a white powder (0.462 g, 35%).

^{1}H-NMR (400 MHz, DMSO-d_6) δ: 10.75 (s, 1H, N^{1}H), 7.94-7.91 (m, 2H, H11), 7.85 (s, 1H, H8), 7.69-7.64 (t, J=7.4 Hz, 1H, H13), 7.52 (dd, J=7.6 Hz, 2H, H12), 6.58 (s, 2H, N^{2}H), 6.06 (d, J=1.9 Hz, 1H, H1′), 5.33-5.26 (m, 2H, H3′ and H2′), 4.55 (dd, J=3.0, 10.2 Hz, 1H, H5′), 4.44-4.37 (m, 2H, H5″ and H4′), 1.54 (s, 3H, HA2/HA3), 1.35 (s, 3H, HA2/HA3); ^{13}C-NMR (125 MHz, DMSO-d_6) δ: 165.85 (C9), 157.10 (C6), 154.13 (C2), 150.89 (C4), 136.54 (C8), 133.88 (C13), 129.74 (C10), 129.66 (C11), 129.16 (C12), 117.45 (C1A), 113.83 (C5), 88.83 (C1′), 84.63 (C4′), 84.18 (C2′), 81.52 (C3′), 65.09 (C5′), 27.46 and 25.89 (CA2 and CA3) ESI-MS: (M+H$^+$)=428.16

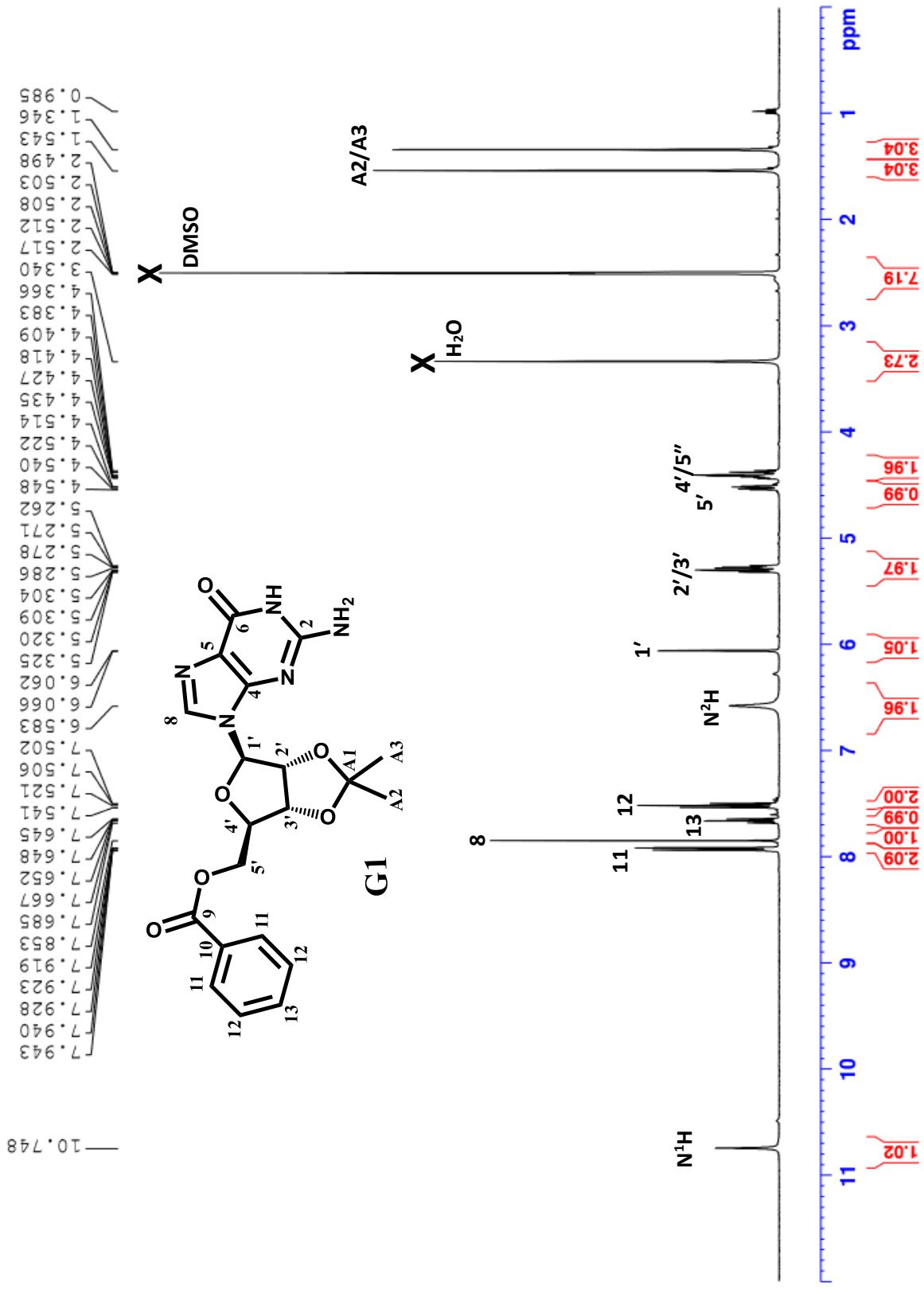

Figure S1. 400 MHz ^{1}H NMR of 5′-benzoyl-2′,3′-isopropylidene guanosine **G1** in DMSO-d_6.

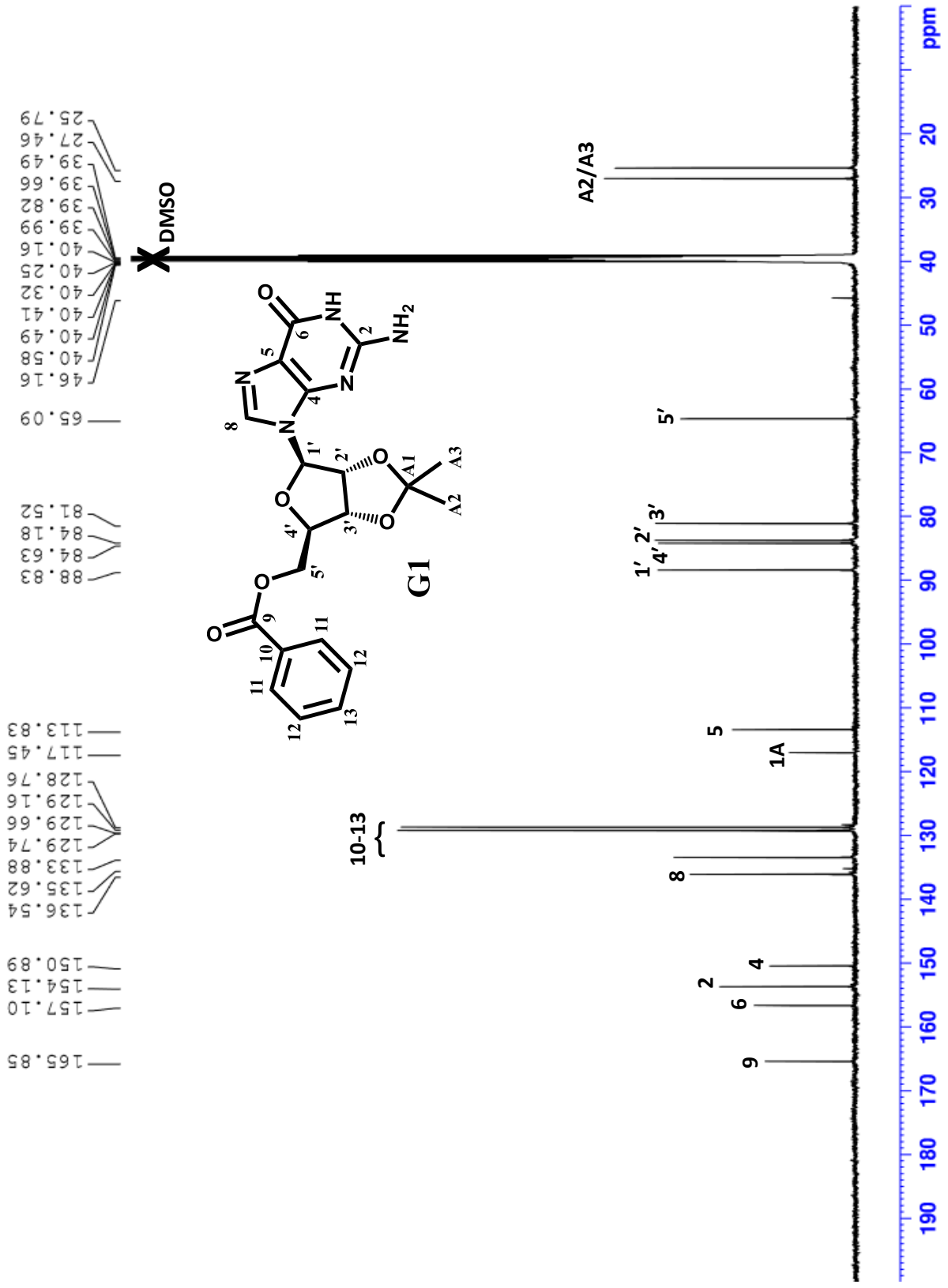

Figure S2. 125 MHz ^{13}C NMR of 5′-benzoyl-2′,3′-isopropylidene guanosine **G1** in DMSO-d_6.

Synthesis of 5′-(4-Nitrobenzoyl)-2′,3′-Isopropylidene Guanosine (G2)

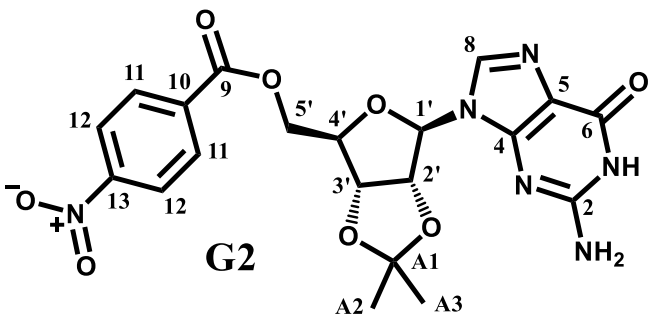

To a suspension of 2′,3′-isopropylideneguanosine (0.50 g, 1.55 mmol), DMAP (15 mg), and triethylamine (0.65 mL, 4.6 mmol) in CH_3CN (18 mL) was added 4-nitrobenzoyl chloride (0.575 g, 3.1 mmol). The reaction mixture was allowed to stir for 4 h, after which time tlc analysis (9:1 CH_2Cl_2:MeOH) indicated the reaction was complete. The reaction mixture was concentrated *in vacuo* to give a white solid. Column chromatography on silica gel (95:5 CH_2Cl_2:MeOH) gave **G2** as a white solid. The solid was washed with water and vacuum dried to give **G2** as a white powder (0.209 g, 28.4 %).

^{1}H-NMR (400 MHz, DMSO-d_6) δ: 10.72 (s,1H, N^{1}H), 8.34-8.31 (m, 2H, H11 or H12), 8.16-8.13 (m, 2H, H11 or H12), 7.85 (s, 1H, H8), 6.57 (s, 2H, N^{2}H), 6.07 (d, J=1.4 Hz, 1H, H1′), 5.32 (m, 2H, H2′ and H3′), 4.61-4.60 (dd, J=5.4, 9.4 Hz, 1H, H5′), 4.46-4.44 (m, 2H, H5′′ and H4′), 1.55 (s, 3H, HA2 or HA3), 1.35 (s, 3H, HA2 or HA3) ^{13}C-NMR (125 MHz, DMSO-d_6) δ: 164.41 (C9), 157.06 (C6), 154.09 (C2), 150.84 (C4), 150.73 (C13), 136.64 (C8), 135.18 (C10), 131.14 (C12), 124.22 (C11), 117.50 (CA1), 113.82 (C5), 88.90 (C1′), 84.57 (C4′), 84.15 (C2′), 81.40 (C3′), 65.77 (C5′), 27.47 and 25.82 (CA2 and CA3) ESI-MS: (M+H$^+$)=473.14

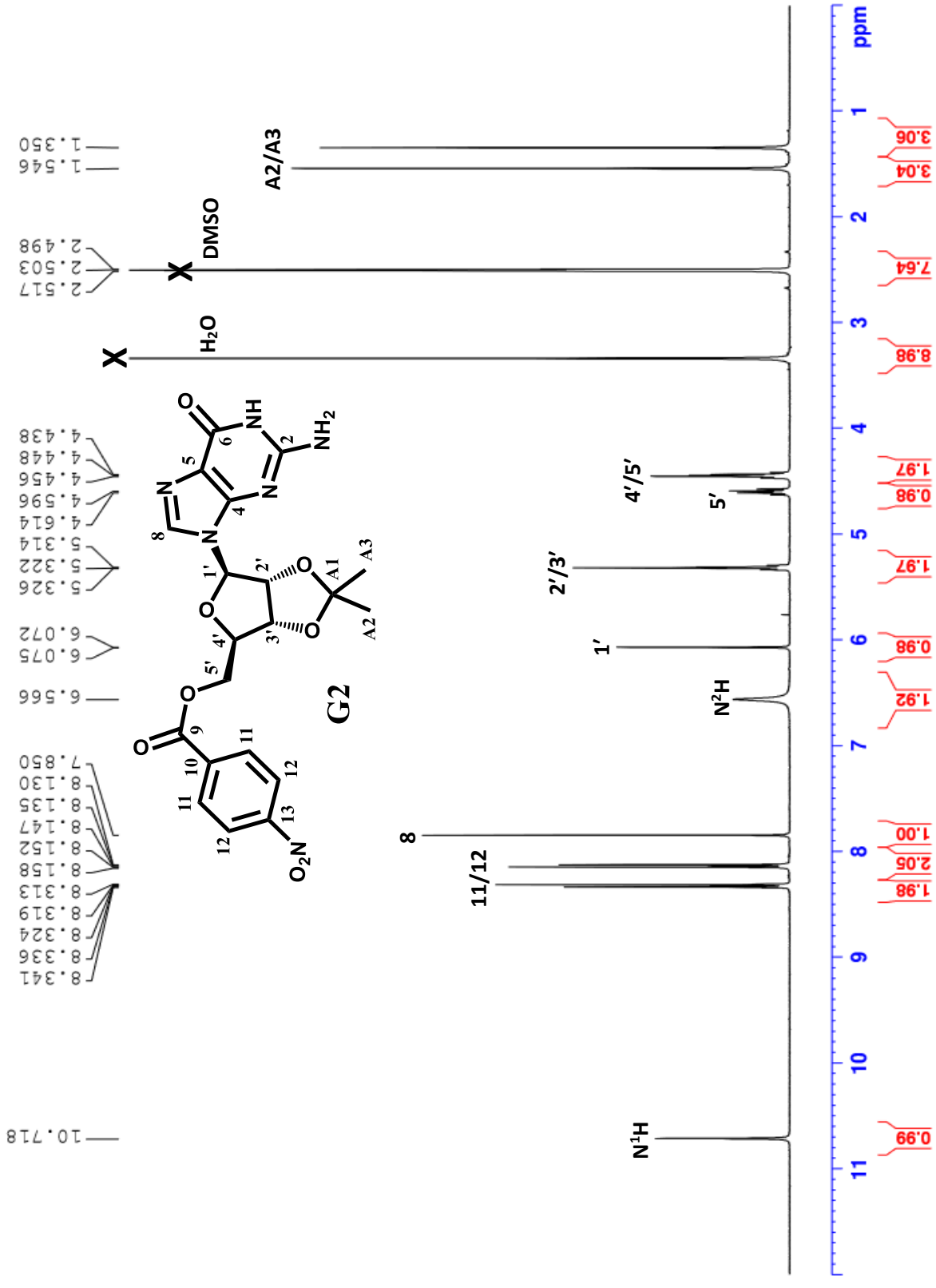

Fig. S3. 400 MHz ^{1}H NMR 5′-(4-nitro)benzoyl-2′,3′-isopropylidene guanosine **G2** in DMSO-d_6.

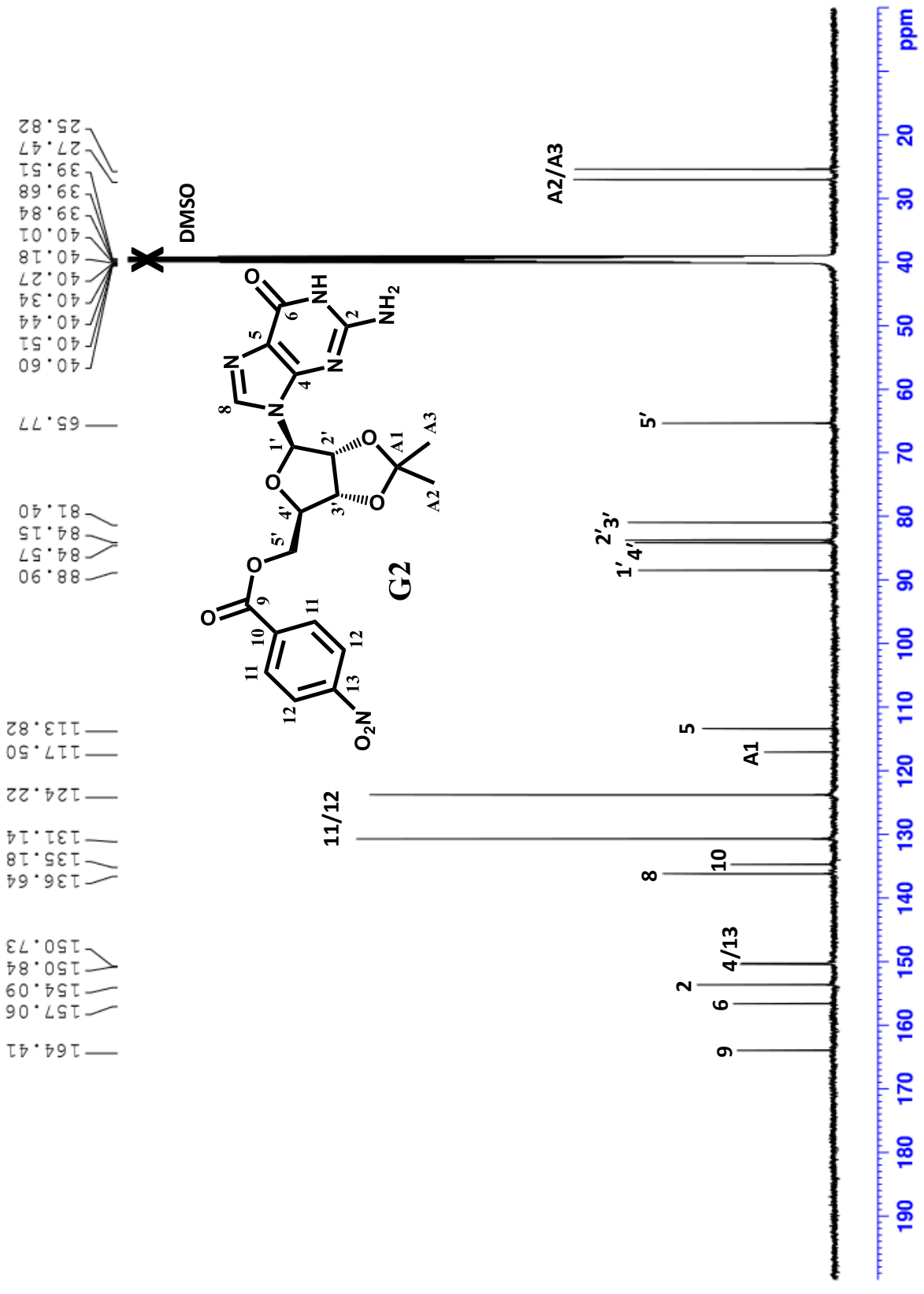

Fig. S4. 125 MHz ^{13}C NMR 5′-(4-nitro)benzoyl-2′,3′-isopropylidene guanosine **G2** in DMSO-d_6.

Synthesis of 5′-(4-Methoxybenzoyl)-2′,3′-Isopropylidene Guanosine (G3)

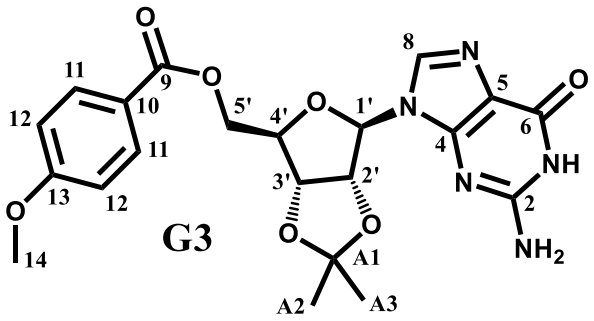

To a suspension of 2′,3′-isopropylideneguanosine (1.00 g, 3.1 mmol), DMAP (27 mg), and triethylamine (1.94 mL, 13.9 mmol) in CH_3CN (18 mL) was added 4-methoxybenzoyl chloride (1.05 mL, 7.7 mmol). The mixture was stirred for 4 h, after which tlc analysis (9:1 CH_2Cl_2:MeOH) indicated that the reaction was complete. The reaction mixture was concentrated *in vacuo* to give a white solid. The resulting solid was triturated with MeOH, filtered and vacuum dried to give **G3** as a white powder (0.532 g, 37.5 %).

^{1}H-NMR (400 MHz, DMSO-d_6) δ: 10.72 (s, 1H, N^{1}H), 7.88-7.86 (d, J=8.9 Hz 2H, H11 or H12), 7.84 (s,1H, H8), 7.04-7.01 (d, J=8.9 Hz, 2H, H11 or H12), 6.56 (s, 2H, N^{2}H$_2$), 6.04 (d, J=2.0 Hz, 1H, H1′), 5.31-5.29 (dd, J=2.0, 6.3 Hz, 1H, H2′), 5.24 (dd, J=3.6, 6.3Hz, 1H, H3′), 4.50 (dd, J=4.1, 11.1 Hz, 1H, H5′), 4.40-4.31 (dt, J=3.7, 7.5 Hz, 1H, H4′), 4.33 (dd, J= 6.6, 11.1 Hz, 1H, H5″), 3.83 (s, 3H, H14), 1.53 (s, 3H, HA2), 1.34 (s, 3H, HA3) ^{13}C-NMR (125 MHz, DMSO-d_6) δ:165.51 (C9), 163.70 (C13), 157.09 (C6), 154.12 (C2), 150.91 (C4), 136.50 (C8), 131.80 (C11), 120.98 (C10), 117.45 (CA1), 114.44 (C12), 113.83 (C5), 88.82 (C1′), 84.65 (C4′), 84.15 (C2′), 81.52 (C3′), 64.76 (C5′), 55.95 (C14), 27.46 and 25.79 (CA2 and CA3) ESI-MS: (M+H$^+$)=458.17

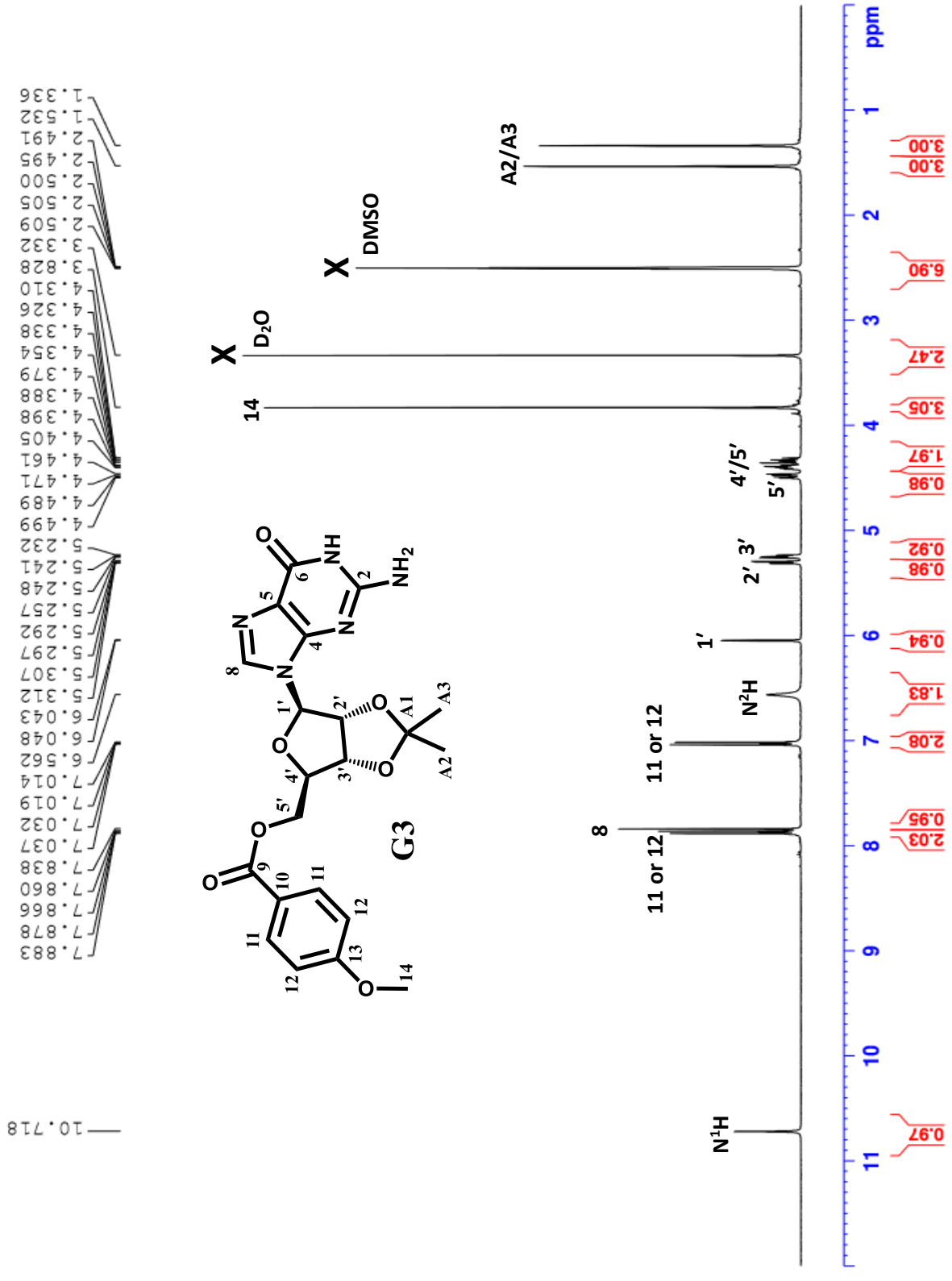

Fig. S5. ^{1}H of NMR 5′-(4-methoxy)benzoyl-2′,3′-isopropylidene guanosine **G3** in DMSO-d_6.

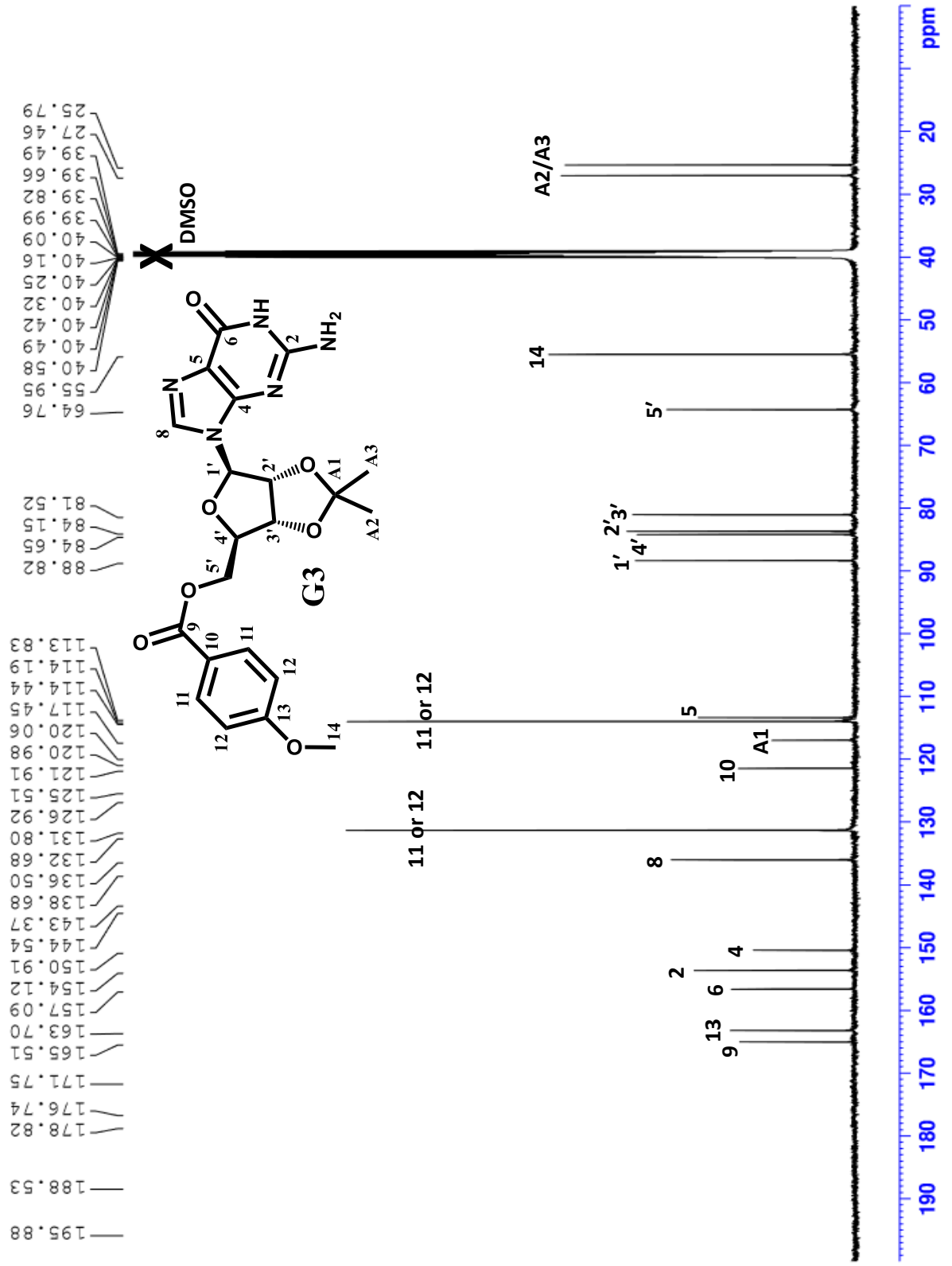

Fig. S6. ^{1}H of NMR 5′-(4-methoxy)benzoyl-2′,3′-isopropylidene guanosine **G3** in DMSO-d_6.

Synthesis of 5′-(2-Naphthoyl)-2′,3′-Isopropylidene Guanosine (G4)

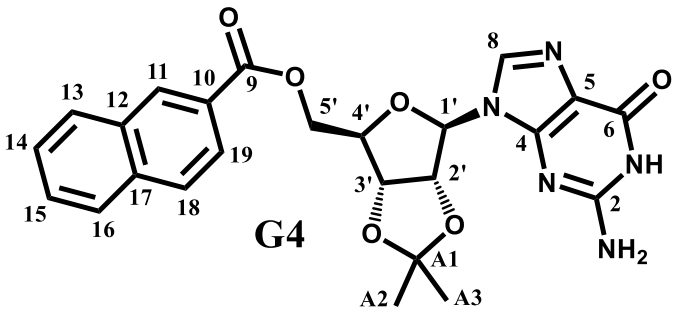

To a suspension of 2′,3′-isopropylideneguanosine (0.50 g, 1.5 mmol), DMAP (20 mg), and triethylamine (0.97 mL, 6.9 mmol) in CH_3CN (18 mL) was added 2-naphthoyl chloride (0.59 g, 3.1 mmol). The reaction mixture was allowed to stir for 4 h, after which time tlc analysis (9:1 CH_2Cl_2:MeOH) indicated the reaction was complete. The product **G4** precipitated out of the reaction mixture as a white powder and was collected by vacuum filtration. The precipitate was washed with water and vacuum dried to give **G4** as a white powder (0.217 g, 29.5%)

^{1}H-NMR (400 MHz, DMSO-d_6) δ: 10.73 (s, 1H, N^1H), 8.58 (t, J=1.0 Hz, 1H), 8.13-8.11 (m, 1H), 8.04 (t, J=7.8 Hz, 2H), 7.96 (dd, J=1.7, 8.6 Hz, 1H), 7.88 (s, 1H, H8), 7.70-7.60 (m, 2H), 6.58 (s, 2H, N^2H_2), 6.09 (d, J=1.1 Hz, 1H, H1′), 5.31 (m, 2H, H2′ and H3′), 4.62 (dd, J=7.7 Hz, 7.8 Hz, 1H, H5′), 4.48-4.45 (m, 2H, H4′ and H5′′), 1.55 (s, 3H, HA2 or HA3), 1.35 (s, 3H, HA2 or HA3); ^{13}C-NMR (125 MHz, DMSO-d_6) δ: 166.0 (C9), 157.10 (C6), 154.15 (C2), 150.91 (C4), 136.54, 135.54, 132.45, 131.09, 129.78, 129.10, 128.82, 128.12, 127.42, 127.05, 125.22, 117.48 (CA1), 113.85 (C5), 88.89 (C1′), 84.82 (C4′), 84.29 (C2′), 81.56 (C3′), 65.39 (C5′), 27.48 and 25.81(CA2 and CA3).

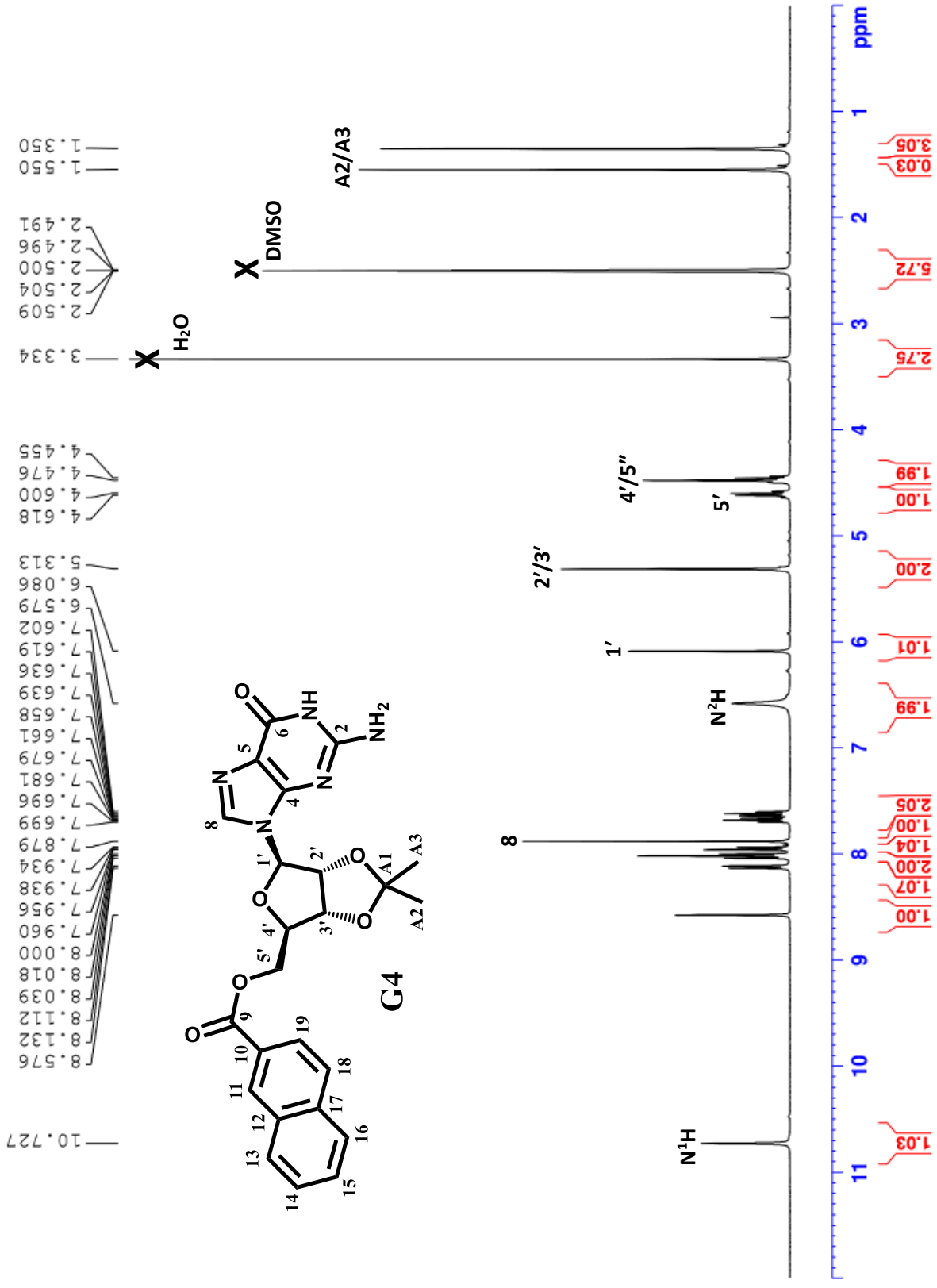

Figure S7. ^{1}H NMR of 5′-naphthoyl-2′,3′-isopropylidene guanosine **G4** in DMSO-d$_6$.

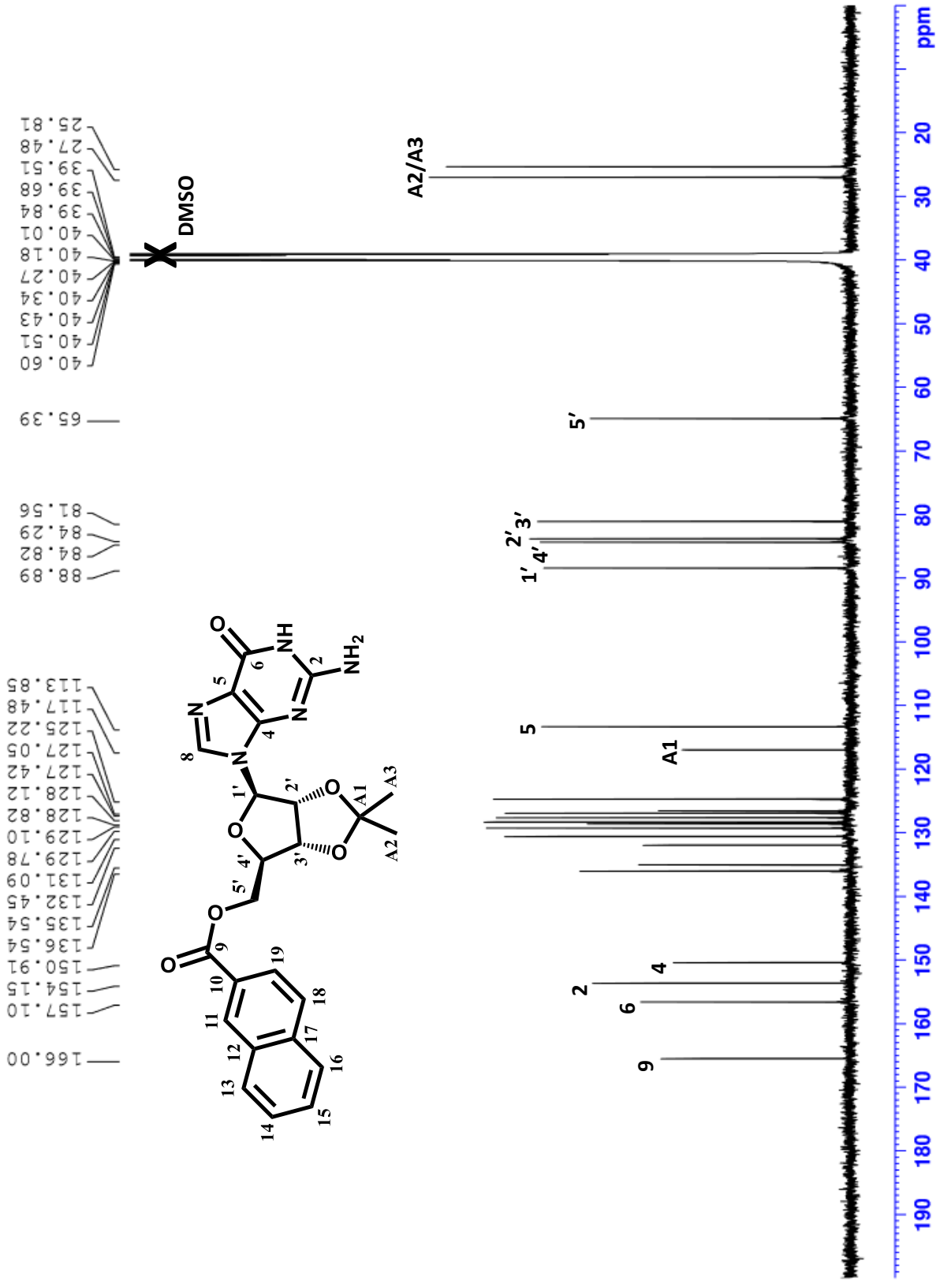

Figure S8. ^{13}C NMR of 5′-naphthoyl-2′,3′-isopropylidene guanosine **G4** in DMSO-d$_6$.

Formation of Octamer $[G]_8 \bullet K^+ I^-$ and Hexadecamer $[G]_{16} \bullet 4K^+ 4I^-$ for NMR Studies. Potassium iodide (0.100 g, 0.602 mmol) was dissolved in H_2O (1 mL) to give a stock solution of 0.602 M KI. Aliquots of the aqueous KI stock solution were added to a clean, dry scintillation vial (2.1 μL to prepare octamer $[G]_8 \bullet K^+ I^-$ or 4.2 μL for hexadecamer $[G]_{16} \bullet 4K^+ 4I^-$) and placed in an oven for 1 h to evaporate the H_2O. A 0.625 mM solution of hexadecamer $[G]_{16} \bullet 4K^+ 4I^-$ or a 1.25 mM solution of octamer $[G]_8 \bullet K^+ I^-$ was prepared in either CD_3CN (1 mL) or $CDCl_3$ (1 mL) by adding 10 mmol of guanosine derivative **G1**-**G4** to the vial containing the appropriate amount of KI, sonicating for one h, and then stirring overnight. The resulting complexes were confirmed by ^1H NMR analysis by their characteristic spectra. The D_4-symmetric octamers $[G]_8 \bullet K^+ I^-$ give a single set of ^1H NMR signals and the D_4-symmetric hexadecamers $[G]_{16} \bullet 4K^+$ give a two sets of ^1H NMR signals of equal intensity, one set for the outer G-quartets and one set for the inner G-quartets. We note that the ^1H NMR spectra of the assemblies made from **G1**-**G4**, be they octamers or hexadecamers, were very similar in both $CDCl_3$ and CD_3CN solvents. Variable temperature experiments (data not shown) suggested that the assemblies were more stable in the less polar $CDCl_3$ than in the more polar solvent CD_3CN. We decided to carry out the DMSO-d_6 titrations (Fig. 2 in the paper) and the H/D exchange experiments (Fig. 3 in the paper) in CD_3CN for 3 reasons: 1) better signal resolution for the 2 amide N^1H protons in CD_3CN; 2) CD_3CN, unlike $CDCl_3$, is miscible with D_2O, which greatly facilitated the H/D exchange experiments and 3) because the hexadecamers are less stable in CD_3CN, than in $CDCl_3$, we could better detect differences in thermodynamic stabilities in the DMSO-d_6 titrations for the hexadecamers made from **G1**, **G3** and **G4**.

Crystallization of Hexadecamer $[G1]_{16} \bullet 3K^+ 3I^-$ To a solution of $[\mathbf{G1}]_{16} \bullet 4K^+ 4I^-$ (0.625 mM) in $CDCl_3$ **(**0.50 mL) was added d_6-benzene (50 μL) as a co-crystallization solvent. The scintillation vial containing this solution was then placed upright, without the lid, into a clean jar that contained Et_2O (5 mL). The jar was capped and stored in a freezer at -6 °C. Yellow, cube-shaped crystals formed after 72 h at -6 °C. Subsequent X-ray analysis showed them to be hexadecamer $[\mathbf{G1}]_{16} \bullet 3K^+ 3I^-$. Crystal Structure data for $[\mathbf{G1}]_{16} \bullet 3K^+ 3I^-$ have been deposited with the Cambridge Crystallographic Data Centre as CCDC-1495606. For some key X-ray crystal data see the information on the following pages S15-S17.

Crystal Structure Experimental and Summary of Hexadecamer $[G1]_{16}$•3K$^+$ 3I$^-$

Crystal structure data for $[\mathbf{G1}]_{16} \bullet 3K^+ 3I^-$ have been deposited with the Cambridge Crystallographic Data Centre as **CCDC-1495606**. Key information is summarized below.

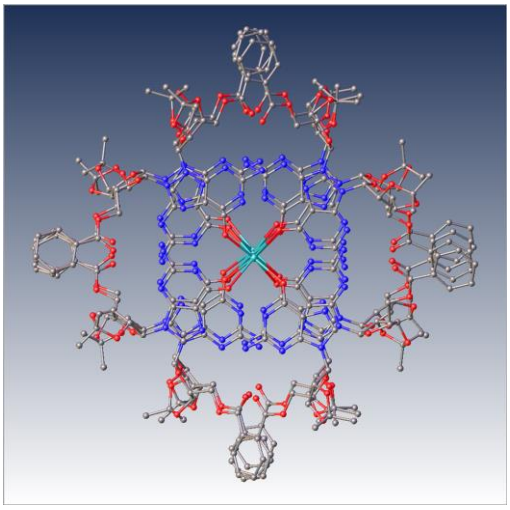

Experimental: A single crystal of UM2749 was selected and measured on a Bruker Smart Apex II CCD diffractometer [1]. The crystal was kept at 200(2) K during data collection. The integral intensity was corrected for absorption with SADABS software [2] using multi-scan method. Resulting minimum and maximum transmission are 0.724 and 0.956 respectively. The structure was solved with the ShelXT program and refined with the XL program and Least Squares minimization using ShelX software [3]. Number of restraints used = 5044, number of constraints - unknown.

Crystal structure determination: *Crystal Data* for $C_{486}H_{510}Cl_{18}I_6K_6N_{120}O_{144}$ (M =11970.21 g/mol): orthorhombic, space group $C222_1$ (no. 20), a = 31.601(7) Å, b = 53.211(12) Å, c = 30.881(7) Å, V = 51927(20) Å^3, Z = 4, T = 200(2) K, μ(MoKα) = 0.599 mm^{-1}, *Dcalc* = 1.531 g/cm^3, 100346 reflections measured ($4.156° \leq 2\Theta \leq 40°$), 24248 unique ($R_{int}$ = 0.1002, R_{sig} = 0.0899) which were used in all calculations. The final R_1 was 0.0784 ($I > 2\sigma(I)$) and wR_2 was 0.2605 (all data).

Refinement details: Disordered solvent was accounted for using SQUEEZE procedure from Platon software (Spek, 1990) but added to the total content in order to obtain more accurate value for density, absorption coefficient and F000. Crystal Structure data for $[\mathbf{G1}]_{16}$•3K$^+$3I$^-$ have been deposited with the Cambridge Crystallographic Data Centre as **CCDC-1495606**.

References:

1. Bruker (2010). Apex2. Bruker AXS Inc., Madison, Wisconsin, USA.
2. Sheldrick, G. M. (2008), Acta Cryst. A64, 112-122.
3. Sheldrick, G. M. (2014). SHELXL-2014. University of Gottingen, Germany.
4. Dolomanov, O.V., Bourhis, L.J., Gildea, R.J, Howard, J.A.K. & Puschmann, H. (2009), J. Appl. Cryst. 42, 339-341.

Table S1. Crystal data and structure refinement for UM2749

Identification code	UM2749
Empirical formula	$C_{486}H_{510}Cl_{18}I_6K_6N_{120}O_{144}$
Formula weight	11970.21
Temperature/K	200(2)
Crystal system	orthorhombic
Space group	$C222_1$
a/Å	31.601(7)
b/Å	53.211(12)
c/Å	30.881(7)
α/°	90
β/°	90
γ/°	90
Volume/Å^3	51927(20)
Z	4
ρ_{calc}g/cm^3	1.531
μ/mm^{-1}	0.599
F(000)	24624.0
Crystal size/mm^3	0.23 × 0.20 × 0.075
Radiation	MoKα (λ = 0.71073)
2Θ range for data collection/°	4.156 to 40
Index ranges	$-30 \leq h \leq 30$, $-51 \leq k \leq 50$, $-29 \leq l \leq 29$
Reflections collected	100346
Independent reflections	24248 [R_{int} = 0.1002, R_{sigma} = 0.0899]
Data/restraints/parameters	24248/5044/2317
Goodness-of-fit on F^2	1.013
Final R indexes [I>=2σ (I)]	R_1 = 0.0784, wR_2 = 0.2055
Final R indexes [all data]	R_1 = 0.1355, wR_2 = 0.2605
Largest diff. peak/hole / e Å^{-3}	0.49/-0.37
Flack parameter	0.041(10)

Table S2. Hydrogen Bonds for UM2749.

Data for the interlayer N^2H_B--O=C H-bonds are indicated in bold.

D	H	A	d(D-H)/Å	d(H-A)/Å	d(D-A)/Å	D-H-A/°
N11A	H11A	O10B	0.88	2.04	2.888(14)	160.4
N13A	**H13A**	**O33F**	**0.88**	**2.32**	**3.192(16)**	**171.0**
N13A	H13B	N17B	0.88	2.05	2.924(15)	170.4
N11B	H11B	O10C	0.88	2.06	2.900(14)	159.7
N13B	**H13C**	**O33G**	**0.88**	**2.16**	**3.044(17)**	**178.2**
N13B	H13D	N17C	0.88	2.06	2.928(16)	168.3
N11C	H11C	O10D	0.88	2.01	2.858(14)	161.3
N13C	**H13E**	**O33H**	**0.88**	**2.31**	**3.184(17)**	**172.3**
N13C	H13F	N17D	0.88	2.04	2.916(16)	171.5
N11D	H11D	O10A	0.88	2.10	2.944(13)	160.3
N13D	**H13G**	**O33E**	**0.88**	**2.13**	**3.014(18)**	**178.5**
N13D	H13H	N17A	0.88	2.05	2.926(15)	170.4
N11E	H11E	O10H	0.88	2.00	2.851(14)	163.4
N13E	**H13I**	**O33D**	**0.88**	**2.24**	**3.116(18)**	**177.6**
N13E	H13J	N17H	0.88	2.11	2.976(16)	166.8
N11F	H11F	O10E	0.88	2.00	2.860(14)	167.0
N13F	**H13K**	**O33A**	**0.88**	**2.16**	**3.038(16)**	**174.9**
N13F	H13L	N17E	0.88	2.07	2.924(15)	164.5
N11G	H11G	O10F	0.88	2.03	2.877(15)	162.5
N13G	**H13M**	**O33B**	**0.88**	**2.20**	**3.077(18)**	**177.4**
N13G	H13N	N17F	0.88	2.09	2.948(16)	164.7
N11H	H11H	O10G	0.88	1.99	2.854(14)	168.7
N13H	**H13O**	**O33C**	**0.88**	**2.13**	**3.007(17)**	**172.3**
N13H	H13P	N17G	0.88	2.12	2.941(16)	155.3

Additional Data

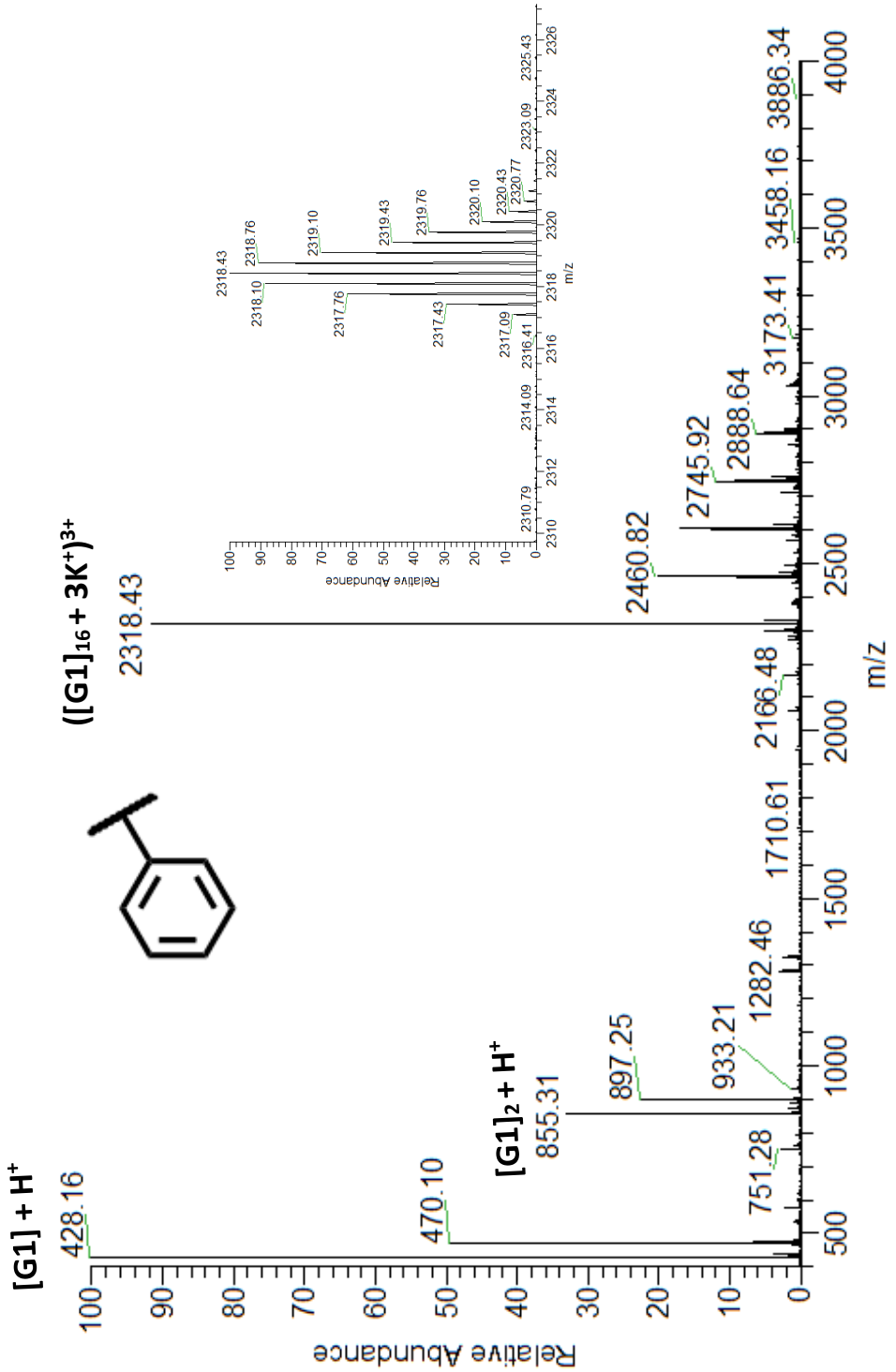

Figure S9. ESI-MS of $[\mathbf{G1}]_{16} \bullet 3K^+ 3I^-$ from $CDCl_3$. The sample was prepared from 10 mM **G1** with 0.25 eq. KI in $CDCl_3$.

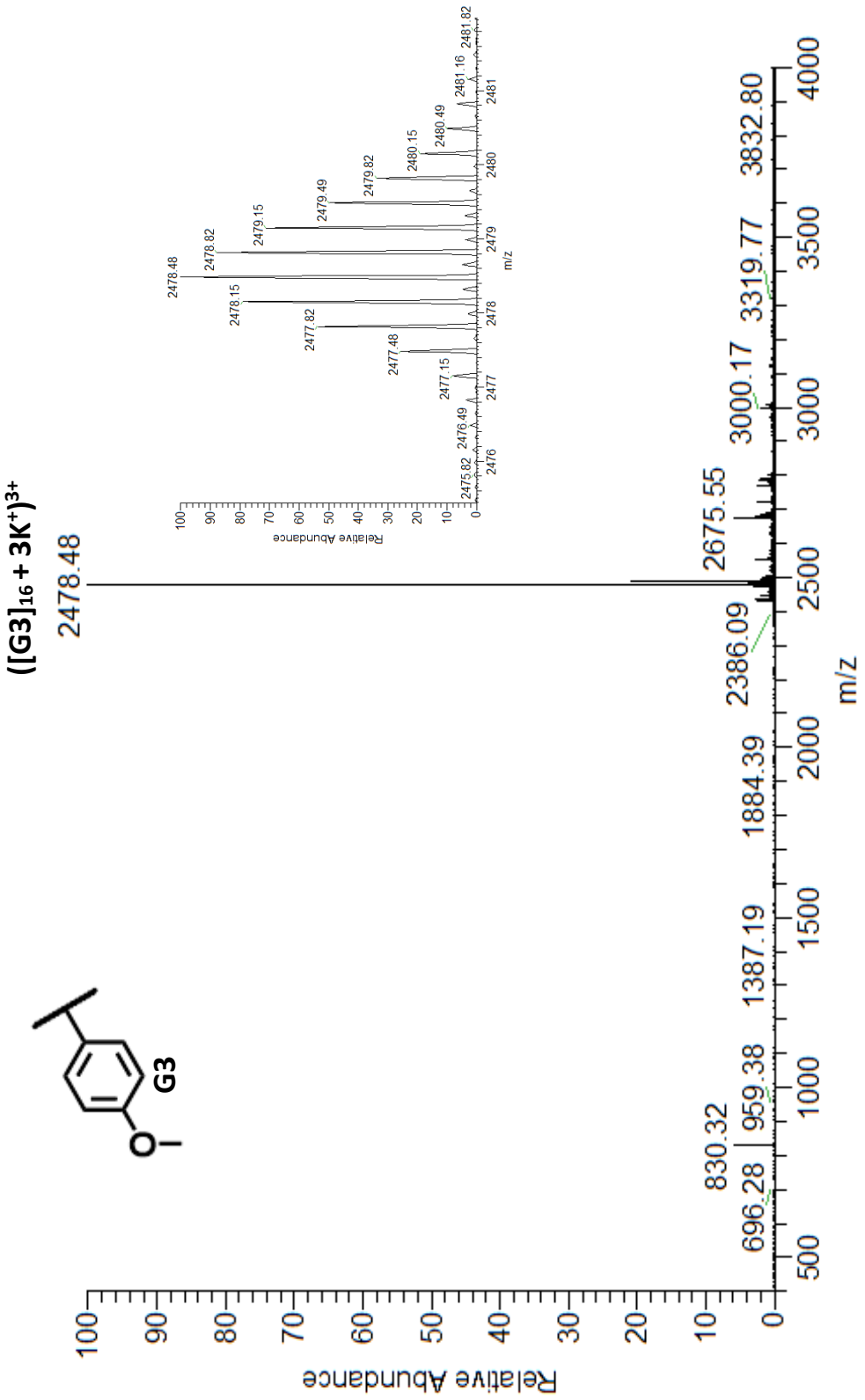

Figure S10. ESI-MS of $[\mathbf{G3}]_{16} \bullet 3K^+ 3I^-$ from $CDCl_3$. The sample was prepared from 10 mM **G1** with 0.25 eq. KI in $CDCl_3$.

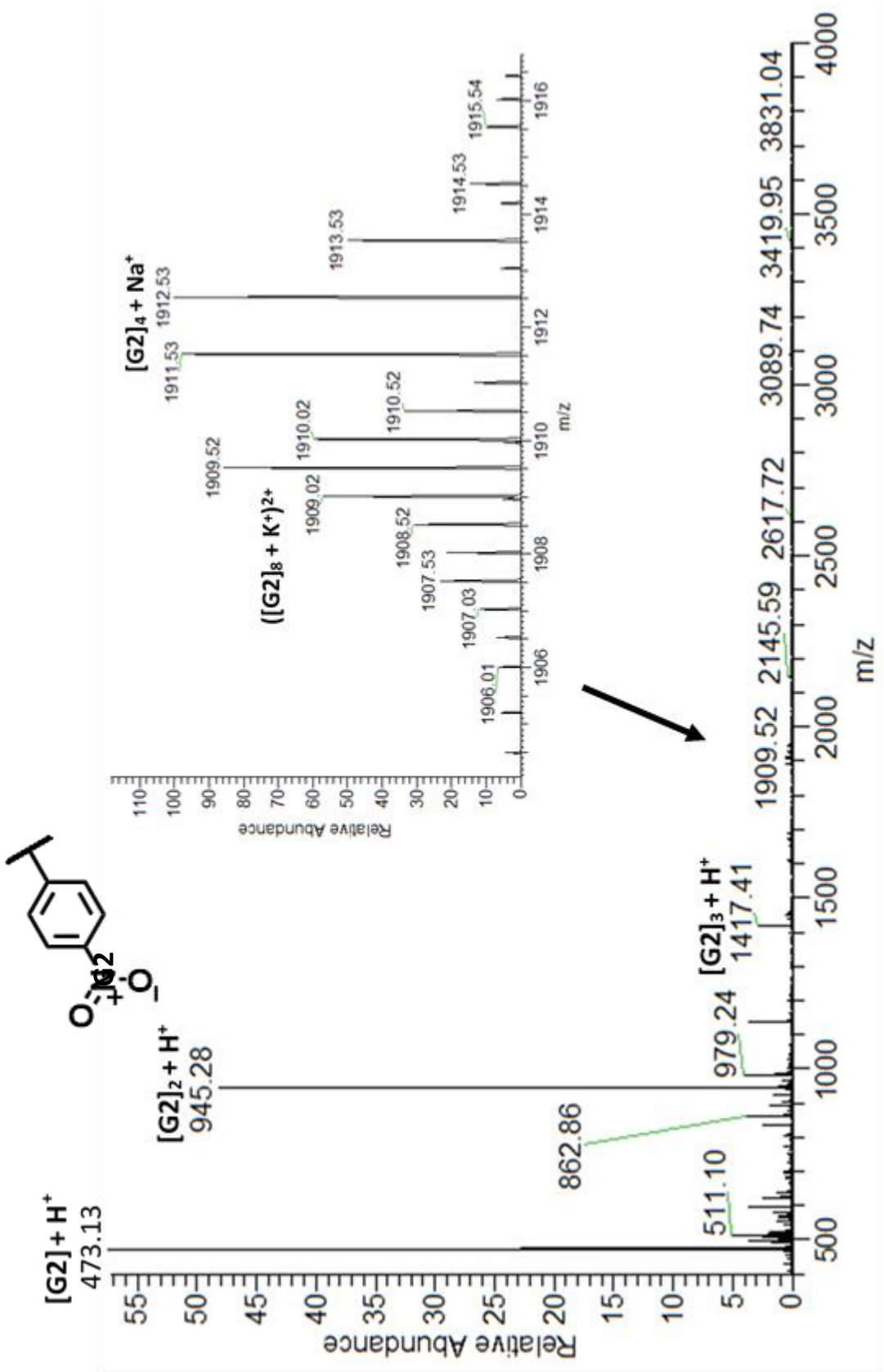

Figure S11. ESI-MS of $[\mathbf{G2}]_8 \bullet K^+ I^-$ from $CDCl_3$. The sample was prepared from 10 mM **G1** with 0.25 eq. KI in $CDCl_3$. The data indicate that this sample contains octamer $[G2]_8 \bullet K^+$ that co-exists with smaller, unchelated aggregates of **G2**.

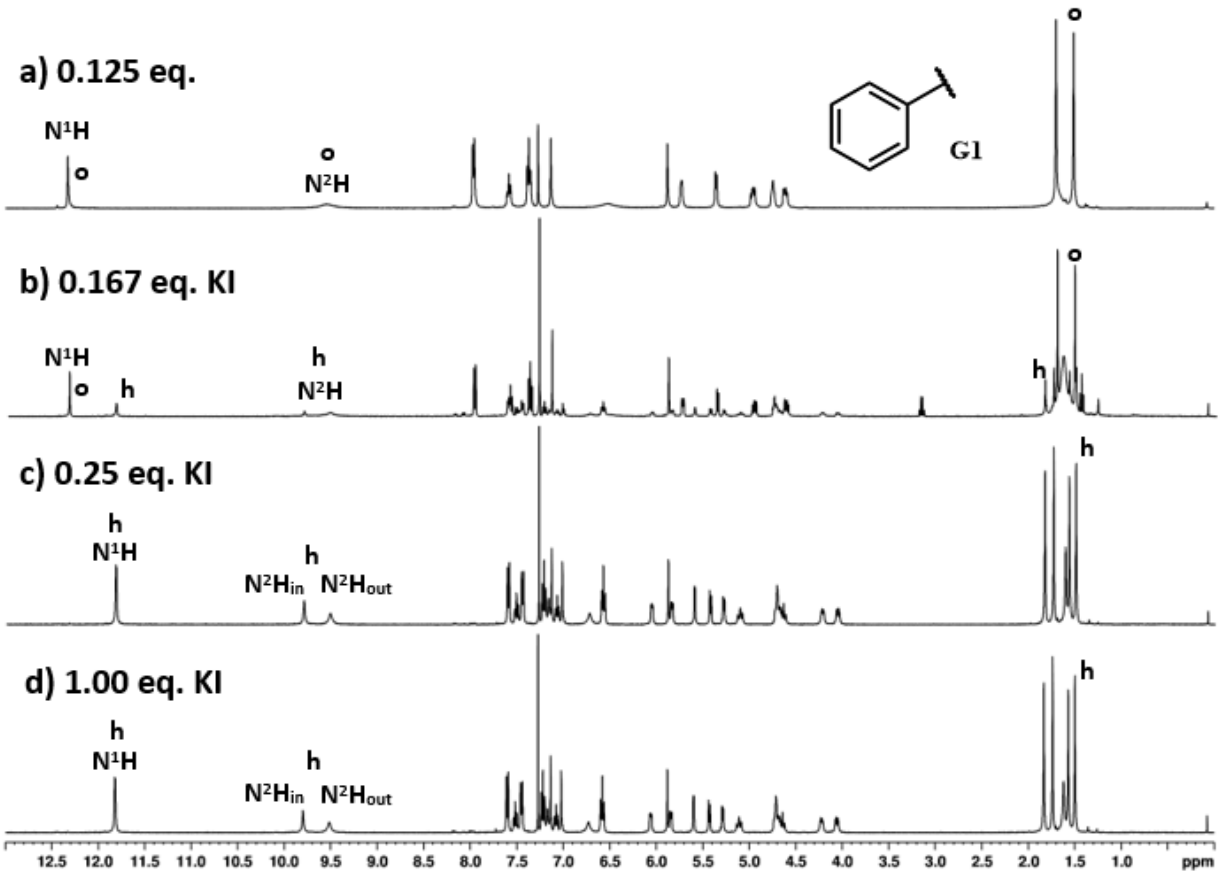

Figure S12. A set of ^{1}H NMR (400 MHz) spectra of 10 mM **G1** in $CDCl_3$ at 25 ^{o}C in the presence of 0.125, 0.167, 0.25, and 1.00 eq of KI. In the top spectrum, with 0.125 eq of KI, a single set of ^{1}H NMR signals are observed, consistent with formation of a D_4-symmetric octamer $[\mathbf{G1}]_8 \bullet K^+ I^-$. In the presence of 0.25 eq of KI the NMR shows 2 sets of signals of equal intensity, consistent with formation of a D_4-symmetric hexadecamer $[\mathbf{G1}]_{16} \bullet 3K^+ 3I^-$. Selected signals for the octamer are labeled (o) and selected signals for the hexadecamer are labeled (h). It should be noted that the amide N^1H signal appears to be a singlet, but in fact the resonances for the outer N^1H and inner N^1H are coincidentally overlapped under these conditions. Changing the temperature or adding co-solvents results in resolution of the overlapped amide N^1H peaks.

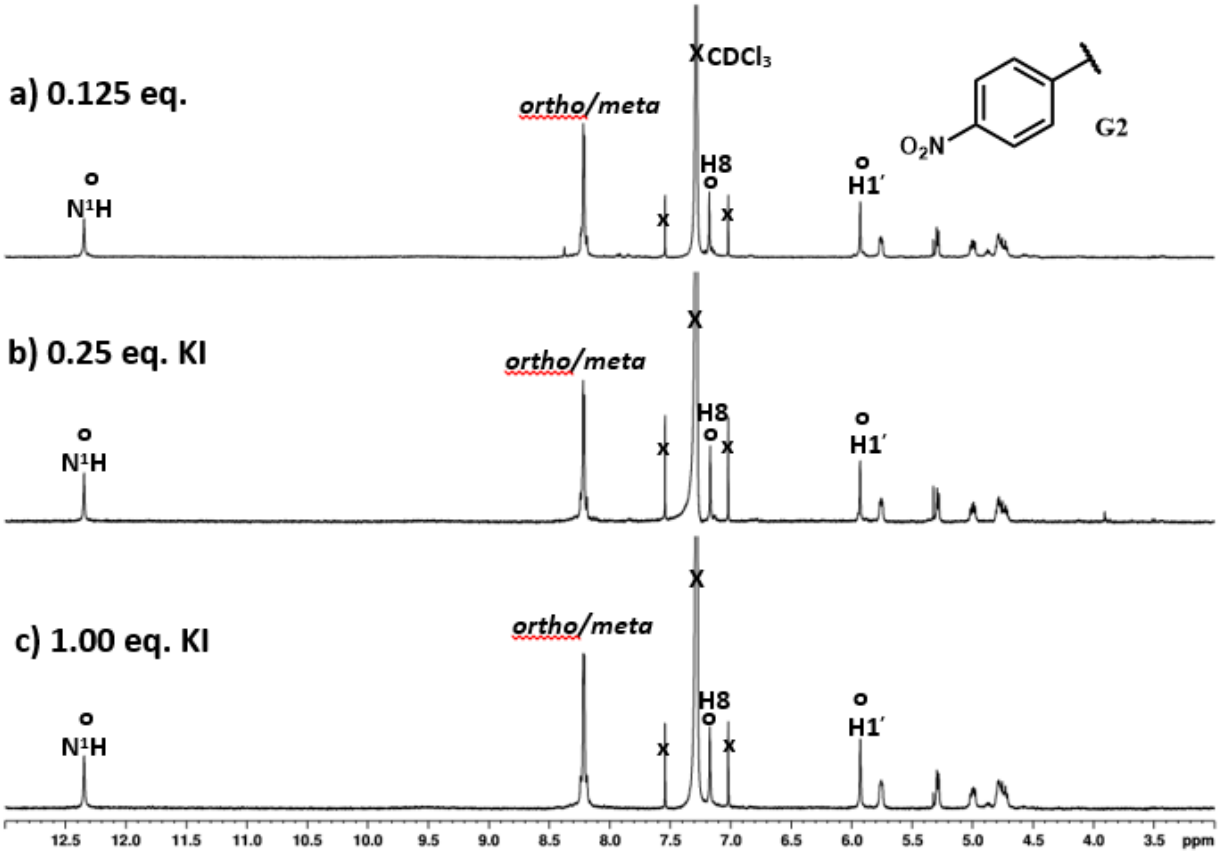

Figure S13. A set of ^{1}H NMR (400 MHz) spectra of 10 mM **G2** in $CDCl_3$ at 25 ^{o}C in the presence of 0.125, 0.25, and 1.00 eq of KI. Under all conditions only a single set of ^{1}H NMR signals are observed, consistent with formation of a D_4-symmetric octamer $[\mathbf{G2}]_8 \bullet K^+ I^-$. In the presence of excess KI the p-nitrobenzoyl ester analog does not form a hexadecamer $[\mathbf{G2}]_{16} \bullet 3K^+ 3I^-$. This NMR data is also consistent with the ESI-MS data in Fig. S11, which shows a weak peak for only octamer and no peak for a hexadecamer. Selected signals in the ^{1}H NMR spectra are labeled (o) for the octamer $[\mathbf{G2}]_8 \bullet K^+ I^-$.

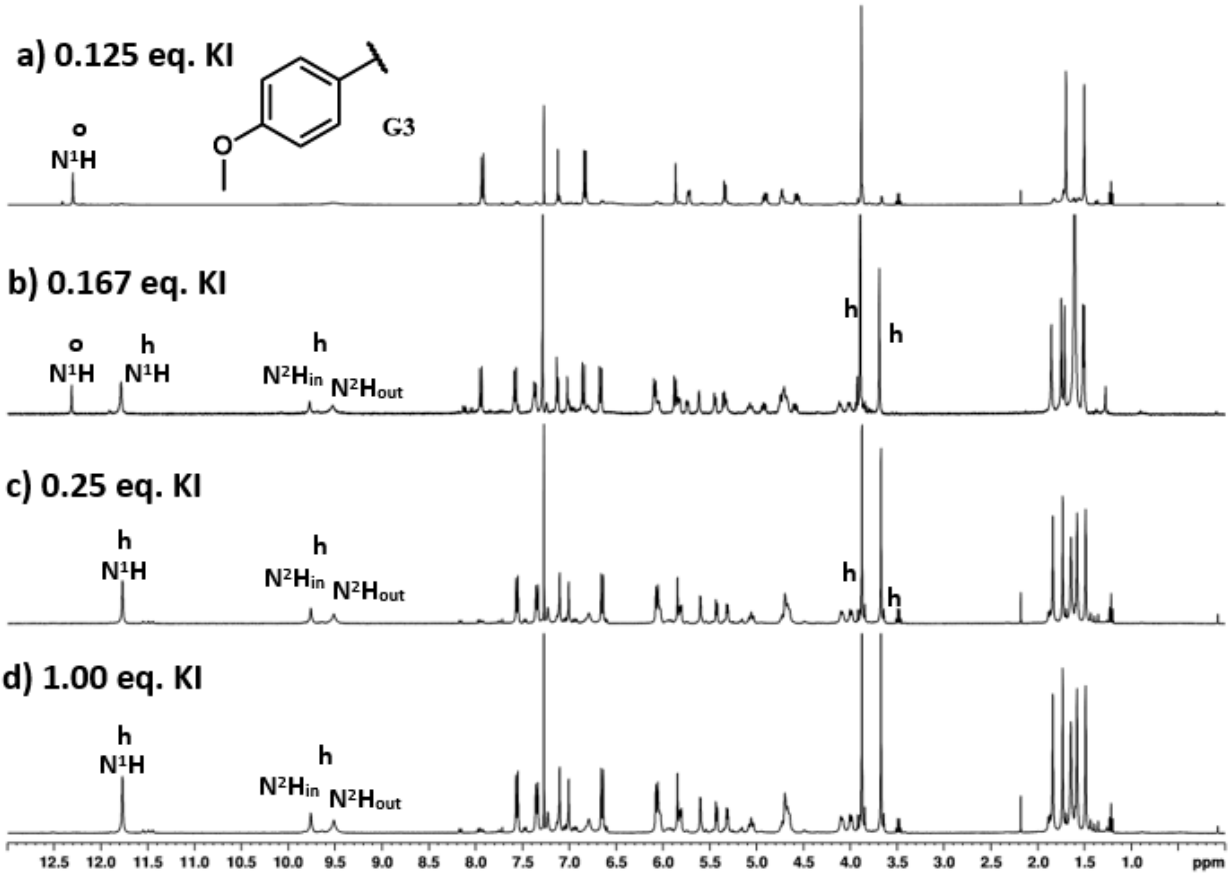

Figure S14. A set of ^{1}H NMR (400 MHz) spectra of 10 mM **G3** in $CDCl_3$ at 25 ^{o}C in the presence of 0.125, 0.167, 0.25, and 1.00 eq of KI. In the top spectrum, with 0.125 eq of KI, a single set of ^{1}H NMR signals are observed, consistent with formation of a D_4-symmetric octamer $[\mathbf{G3}]_8 \bullet K^+ I^-$. In the presence of 0.25 eq of KI the NMR shows 2 sets of signals of equal intensity, consistent with formation of a D_4-symmetric hexadecamer $[\mathbf{G3}]_{16} \bullet 3K^+ 3I^-$. Selected signals for the octamer are labeled (o) and selected signals for the hexadecamer are labeled (h). It should be noted that the amide N^1H signal appears to be a singlet for the hexadecamer $[\mathbf{G3}]_{16} \bullet 3K^+ 3I^-$ in spectra b-d, but in fact the resonances for the outer N^1H and inner N^1H in the hexadecamer are coincidentally overlapped under these conditions. Changing the temperature or adding co-solvents results in resolution of the overlapped amide N^1H peaks.

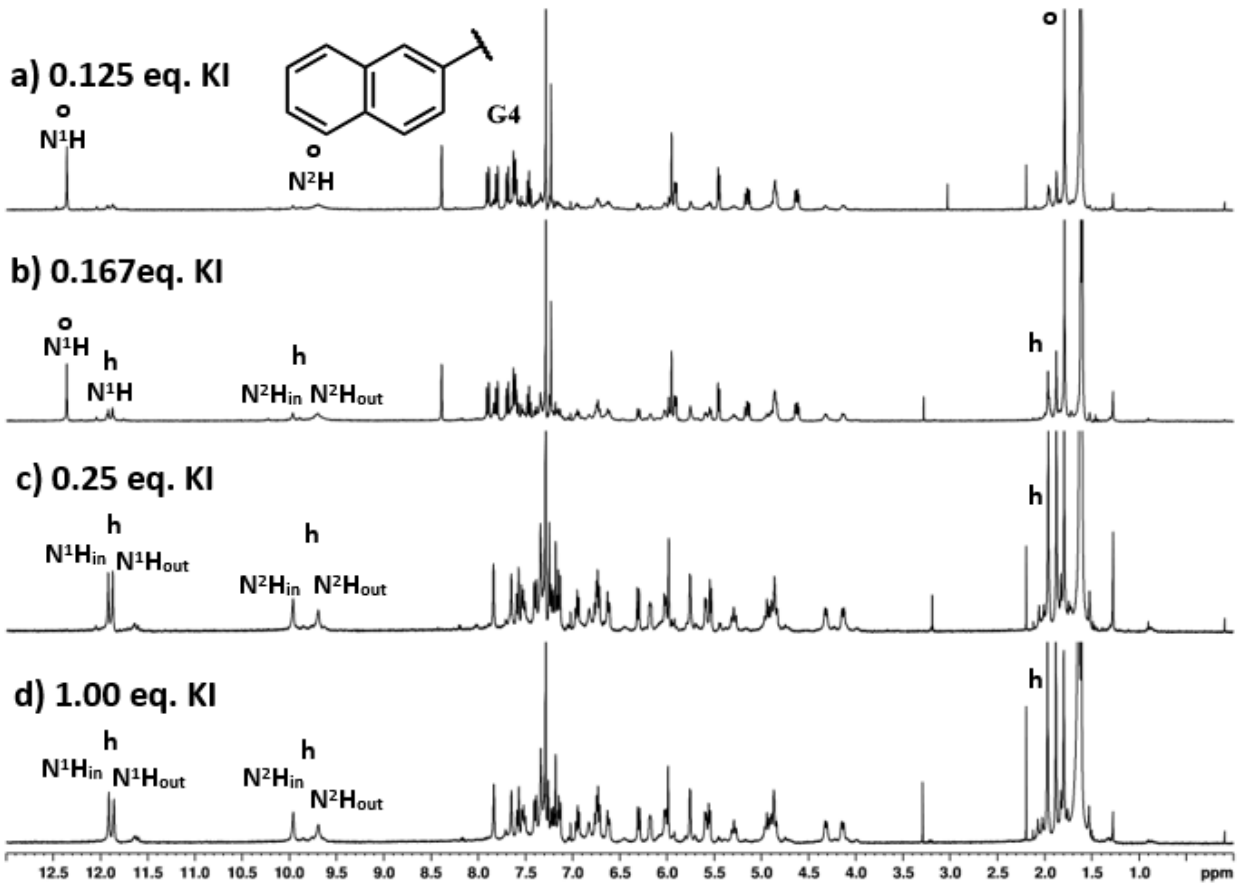

Figure S15. A set of ^{1}H NMR (400 MHz) spectra of 10 mM **G4** in $CDCl_3$ in the presence of 0.125, 0.167, 0.25, and 1.00 eq of KI. In the top spectrum, with 0.125 eq of KI, a single set of ^{1}H NMR signals are observed, consistent with formation of a D_4-symmetric octamer $[\mathbf{G3}]_8 \bullet K^+ I^-$. In the presence of 0.25 eq of KI the NMR shows 2 sets of signals of equal intensity, consistent with formation of a D_4-symmetric hexadecamer $[\mathbf{G4}]_{16} \bullet 3K^+ 3I^-$. Selected signals for the octamer are labeled (o) and selected signals for the hexadecamer are labeled (h).

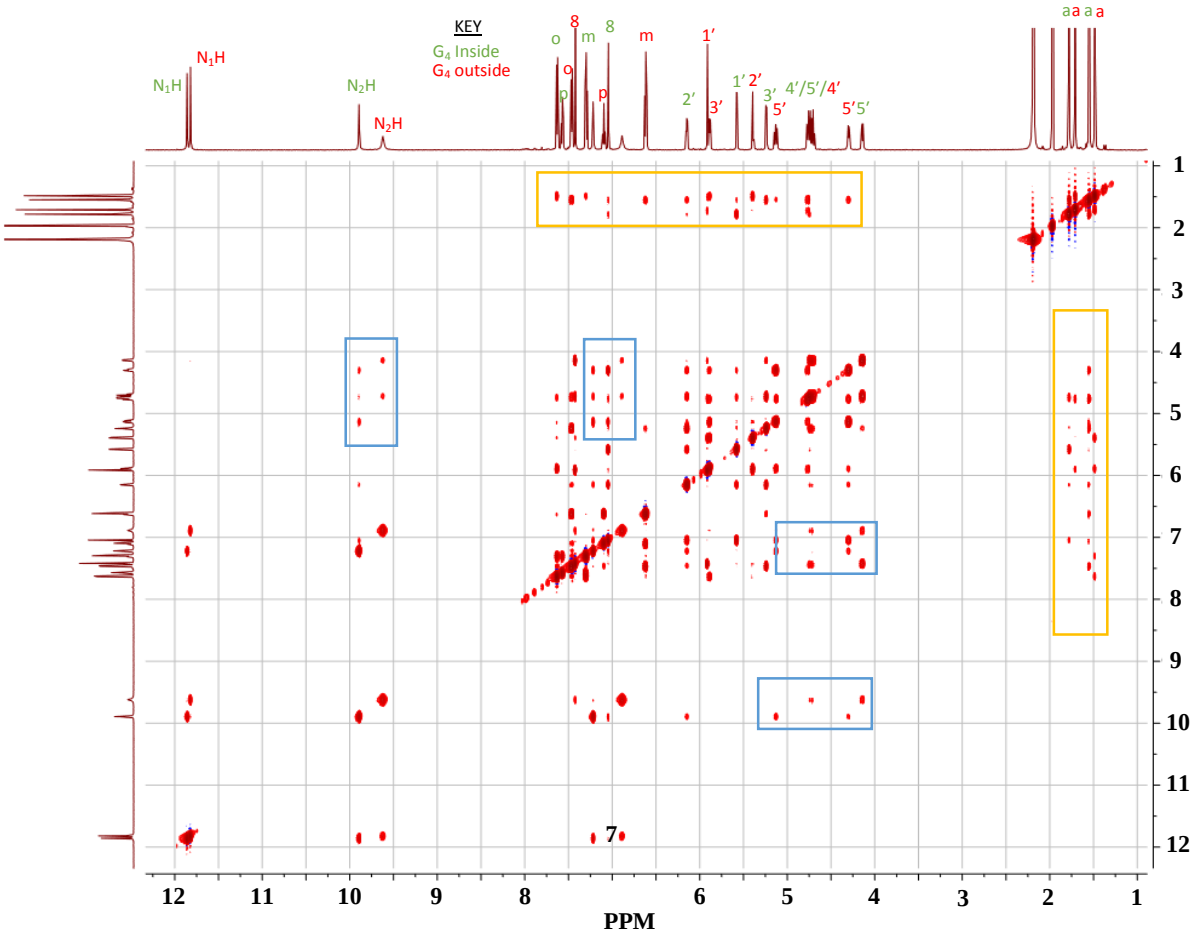

Figure S16. NOESY Spectra for [**G1**]$_{16}$•3K$^+$ hexadecamer in CD_3CN at 25°C. The blue boxes highlight NOE interactions between the H5′,5″ protons and the exocyclic N^2H_A and N^2H_B amino proton. This is significant because it shows that the carbonyl at the 5′-position is in close proximity to the N^2H amino protons of the other layer, consistent with the interlayer N^2H_B--O=C H-bonds seen in the X-ray crystal structure (Table S2). The orange box highlights the interaction of the 2′, 3′-isopropylidene methyl protons of one layer interacting with the benzoyl protons of another layer, further confirming interactions between layers. This data is consistent with the [**G1**]$_{16}$•3K$^+$ hexadecamer crystal structure.

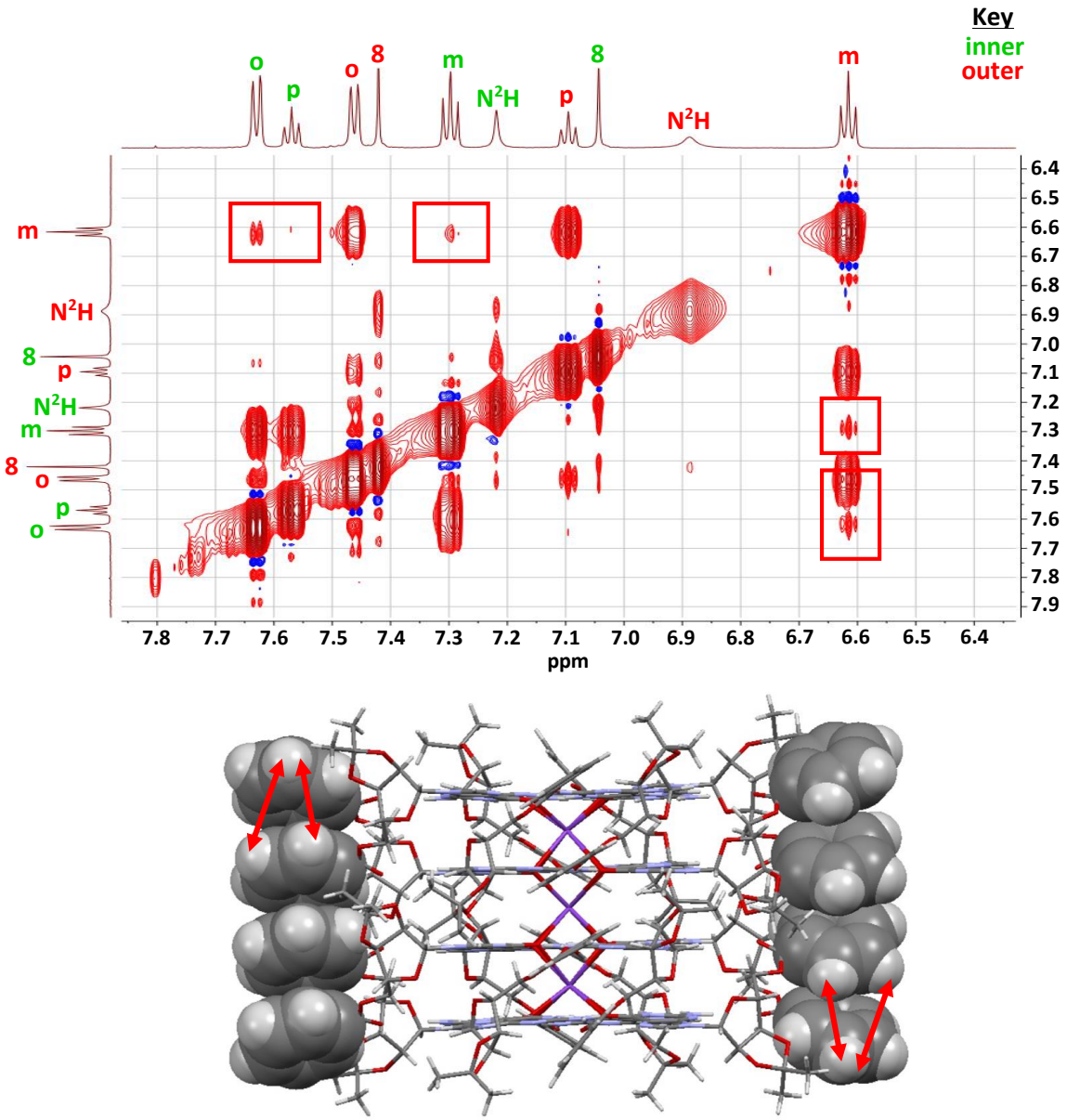

Figure S17. NOE Spectra for [**G1**]$_{16}$•3K$^+$3I$^-$ hexadecamer in CD_3CN at 25°C. The red boxes and arrows highlight the interactions between the benzoyl meta proton of the outer G-quartet with the benzoyl ortho and meta proton of the inner G-quartet. This is significant because it shows that the benzoyl groups are stacking in solution. This data is consistent with the [**G1**]$_{16}$•3K$^+$ hexadecamer crystal structure.

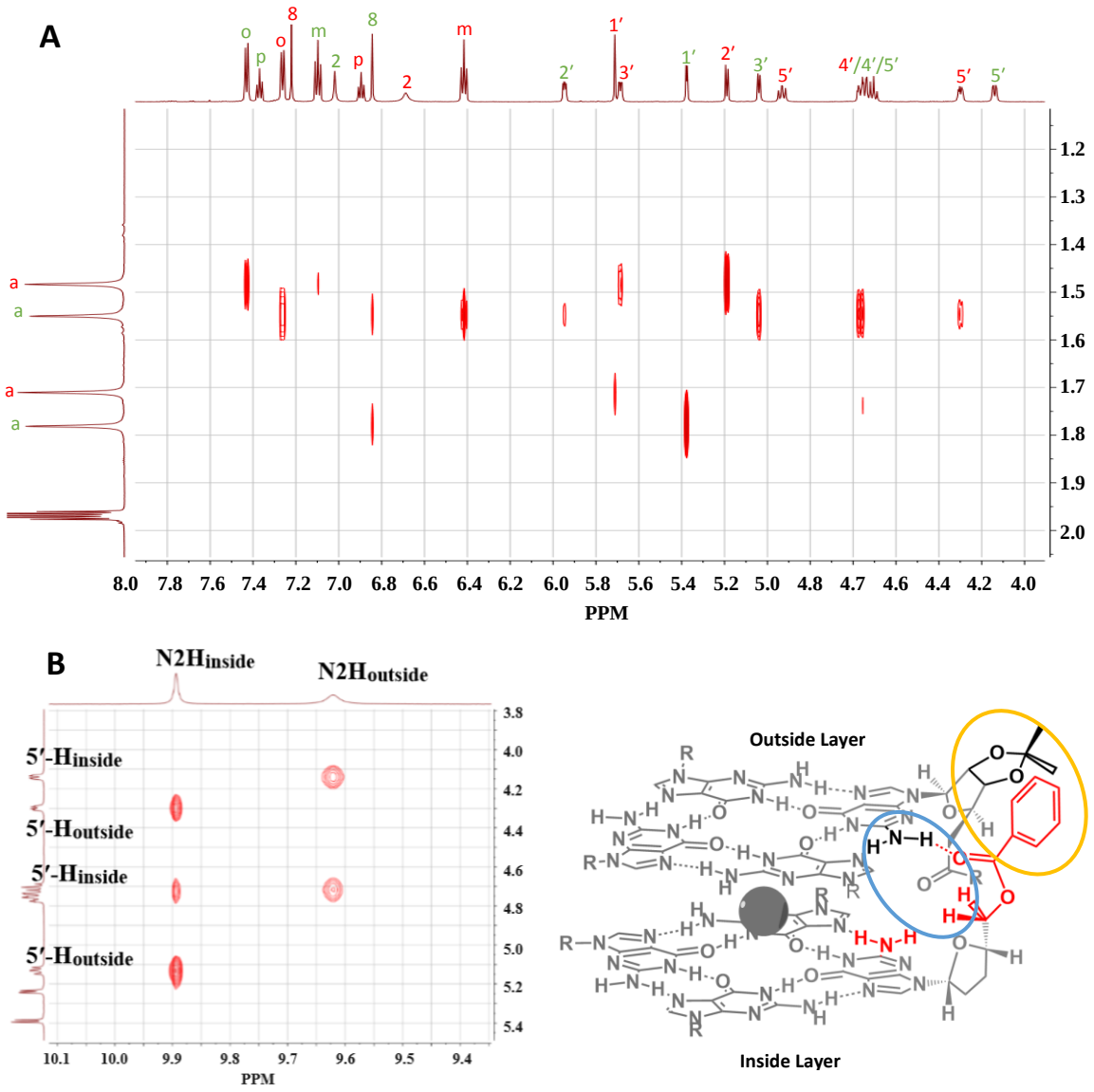

Figure S18. a) NOE Spectra for $[\mathbf{G1}]_{16}\bullet 3K^{+}$ hexadecamer in CD_3CN at 25°C showing the interaction between acetonide protons of the outer G-quartet and the benzoyl protons of the outer G-quartet. **b)** NOE Spectra for $[\mathbf{G1}]_{16}\bullet 3K^{+}$ hexadecamer in CD_3CN at 25°C showing the interaction between N^2H protons of the outer and inner G-quartet and the 5′/5″ protons of the outer G-quartet. These results are consistent with the crystal structure.

Table S3. Chemical Shifts for **G1** Monomer in DMSO-d_6 and [**G1**]$_{16}$•3K$^+$3I$^-$ in CD_3CN

	G1 Monomer DMSO-d_6	**G1$_{16}$-Hexadecamer**			
		Inner G$_4$-quartet	**Δδ**	**Outer G$_4$-Quartet**	**Δδ**
H1′	6.05	5.76	- 0.29	5.91	- 0.14
H2′	5.27	6.14	+ 0.87	5.39	+ 0.12
H3′	5.27	5.24	- 0.03	5.88	+ 0.61
H4′	4.32	4.73	+ 0.41	4.73	+ 0.41
H5′	4.52	4.73	+ 0.21	5.13	+ 0.61
H5″	4.32	4.13	- 0.19	4.30	- 0.02
H8	7.85	7.04	- 0.81	7.41	- 0.44
N^{1}H	10.73	11.86	+ 1.13	11.82	+ 1.09
N^{2}H$_A$	7.94	9.89	+ 1.95	9.62	+ 1.68
N^{2}H$_B$	6.56	7.22	+ 0.66	6.89	+ 0.33
Ortho	7.94	7.63	- 0.31	7.46	- 0.48
Meta	7.51	7.30	- 0.21	6.61	- 0.90
Para	7.65	7.57	- 0.08	7.11	- 0.54

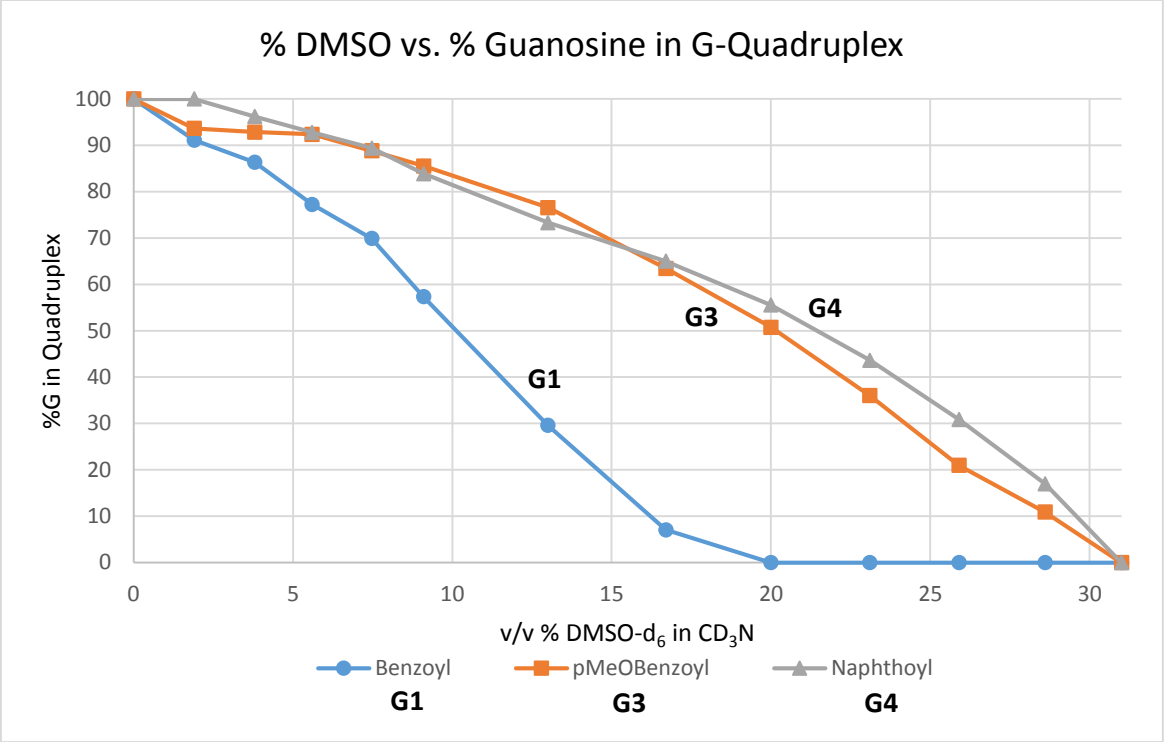

Figure S19. Plot of vol/vol % DMSO-d_6 in CD_3CN versus percentage of guanosine monomer **G1**-**G3** that is bound in the hexadecamers $[\mathbf{G1}]_{16}\bullet 3K^{+}3I^{-}$, $[\mathbf{G3}]_{16}\bullet 3K^{+}3I^{-}$, and $[\mathbf{G4}]_{16}\bullet 3K^{+}3I^{-}$. In this mixed solvent system the ^{1}H NMR resonances for the intact hexadecamer and for any dissociated monomer are in slow exchange on the chemical shift time scale. We integrated the $N^{1}H$ amide signals for the respective hexadecamers $[\mathbf{G}]_{16}\bullet 3K^{+}3I^{-}$ and for G monomer to calculate the % of monomer that remained bound in the hexadecamer at a specific % of DMSO-d_6. See Figs. S20-22 for some of the raw data from these DMSO-d_6 titrations.

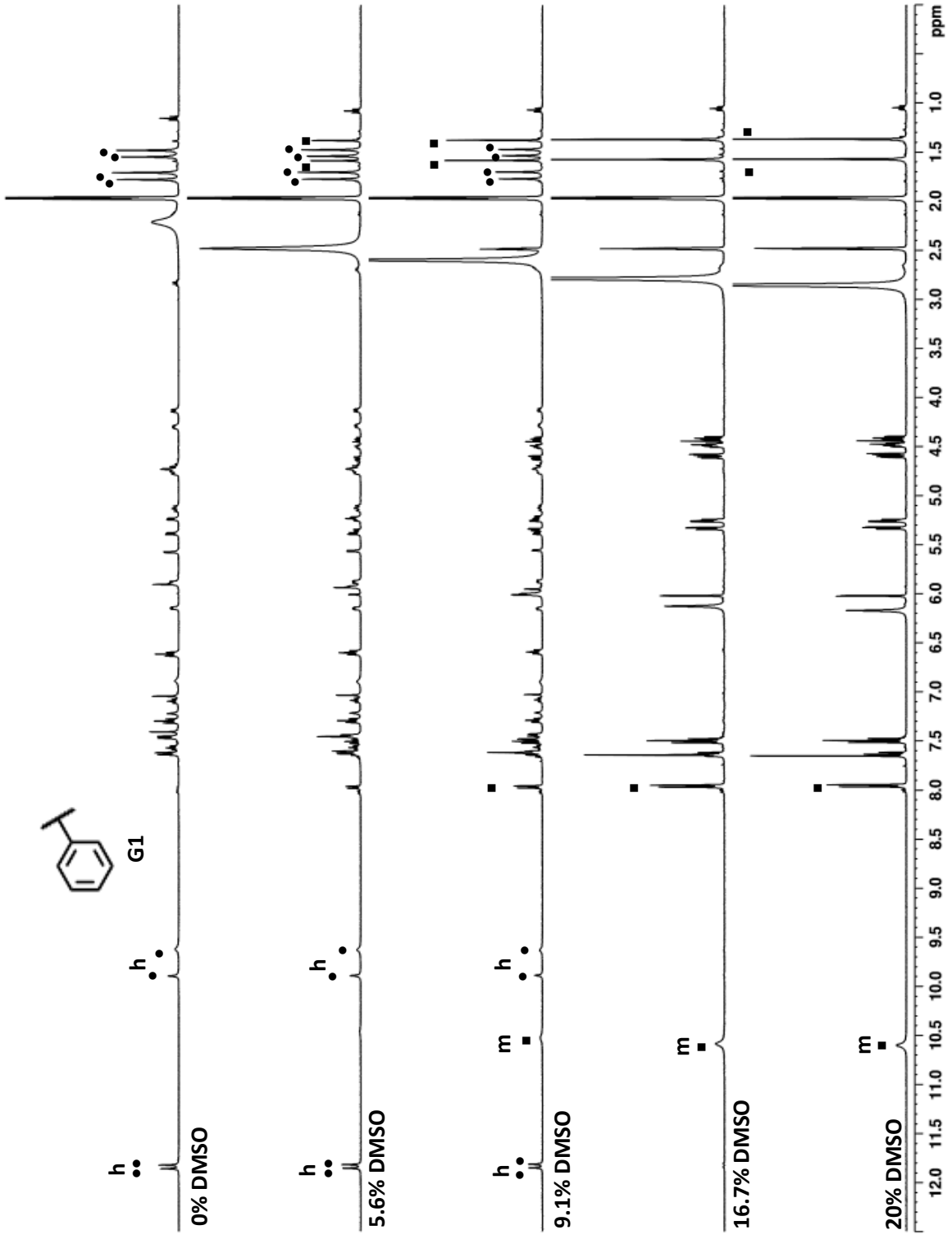

Figure S20. DMSO-d_6 titration of [**G1**]•$3K^+3I^-$ in CD_3CN. Hexadecamer (●, h); Monomer(■,m)

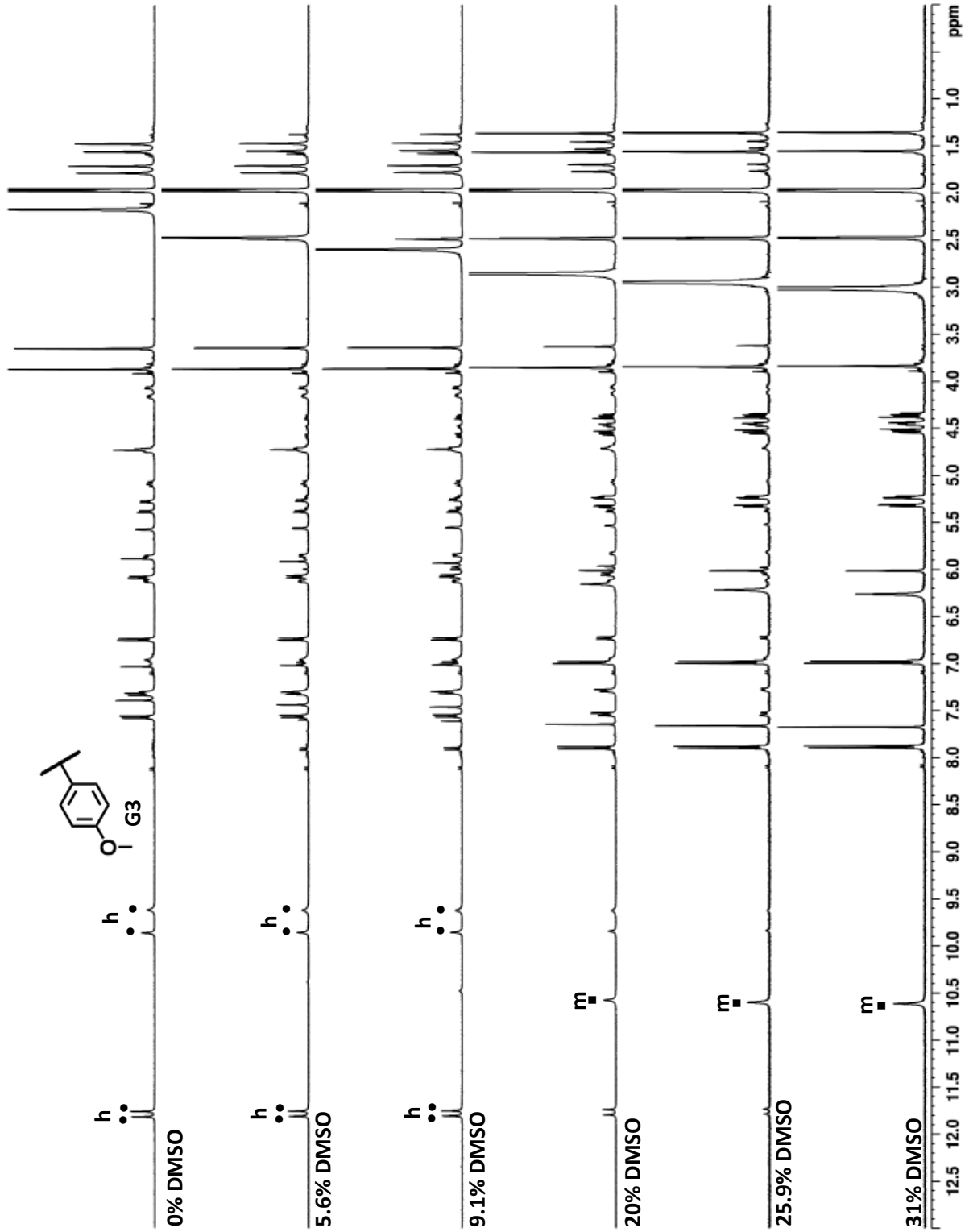

Figure S21. DMSO-d_6 titration of [**G3**]•$3K^+3I^-$ in CD_3CN. Hexadecamer (●, h); Monomer(■,m)

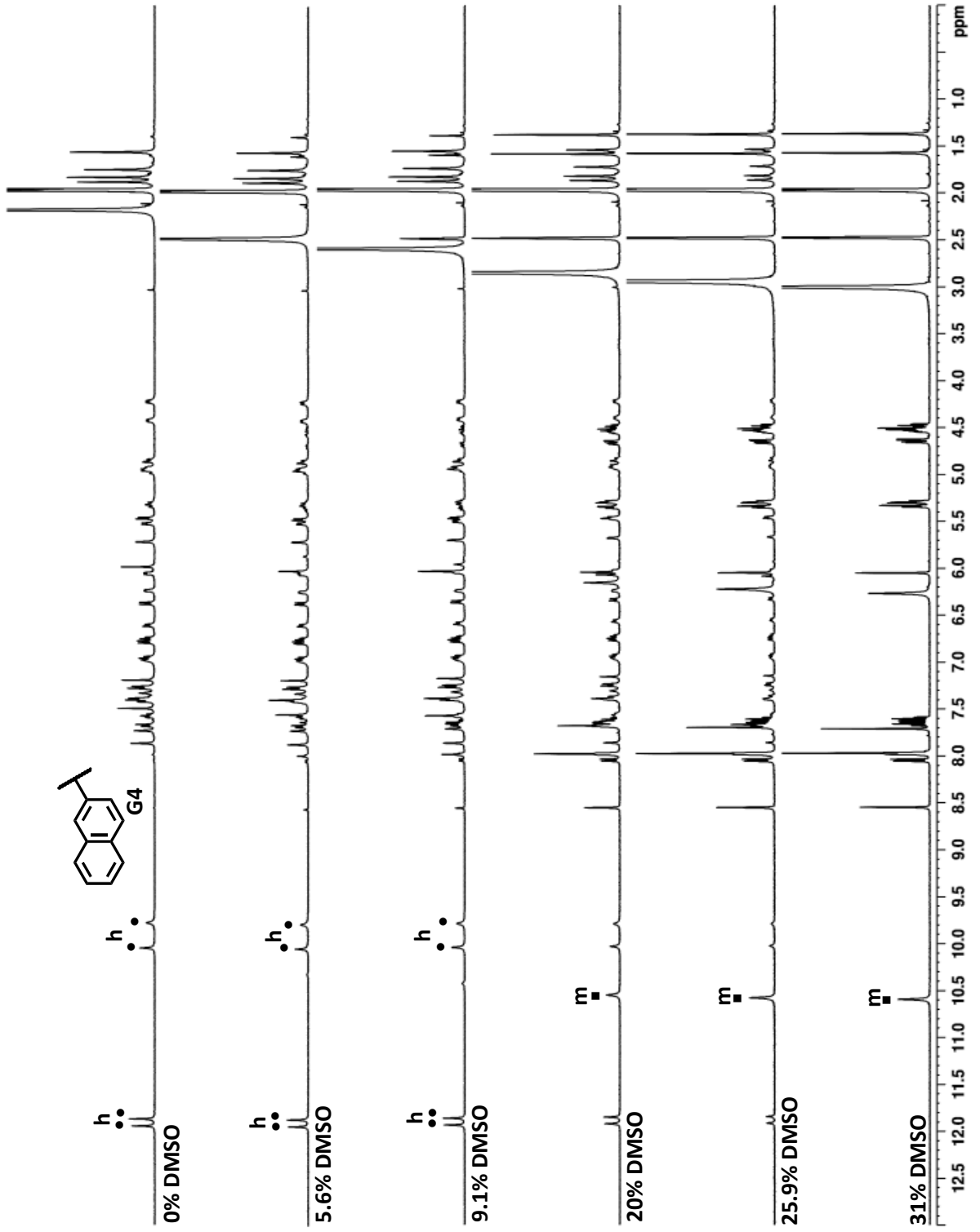

Figure S22. DMSO-d_6 titration of [**G4**]•$3K^+3I^-$ in CD_3CN. Hexadecamer (●, h); Monomer(■,m)

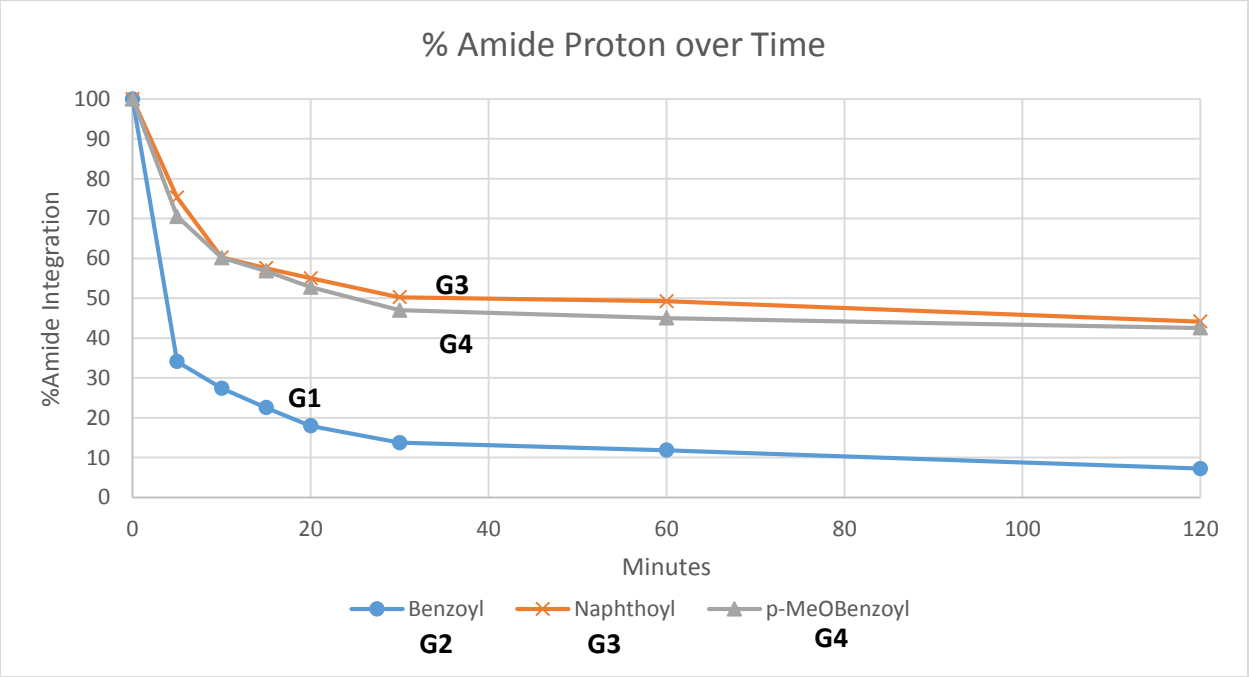

Figure S23. Plot of percentage of amide N^1H proton signal in $[\mathbf{G1}]_{16}\bullet 3K^+3I^-$, $[\mathbf{G3}]_{16}\bullet 3K^+3I^-$, and $[\mathbf{G4}]_{16}\bullet 3K^+3I^-$ over time after addition of 10 μL of D_2O to a solution of the respective G_{16} hexadecamer (0.625 mM) in CD_3CN.

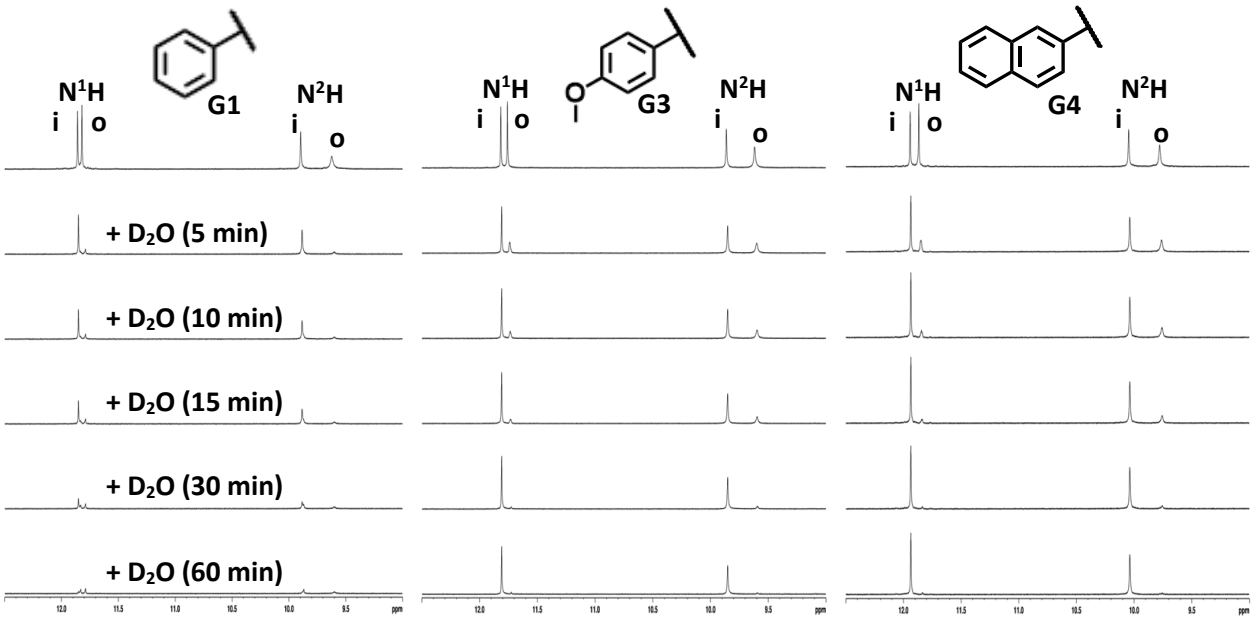

Figure S24. Time dependent H/D exchange for the amide N^1H and amino N^2H protons of $[\mathbf{G1}]_{16}\bullet 3K^+3I^-$ (0.625 mM) in CD_3CN after addition of 10 μL D_2O. The top specrum in each column shows the N^1H/N^2H region before addition of D_2O. The protons in the inner G-quartets are labeled as (i) and protons in the outer G-quartets are labeled as (o).

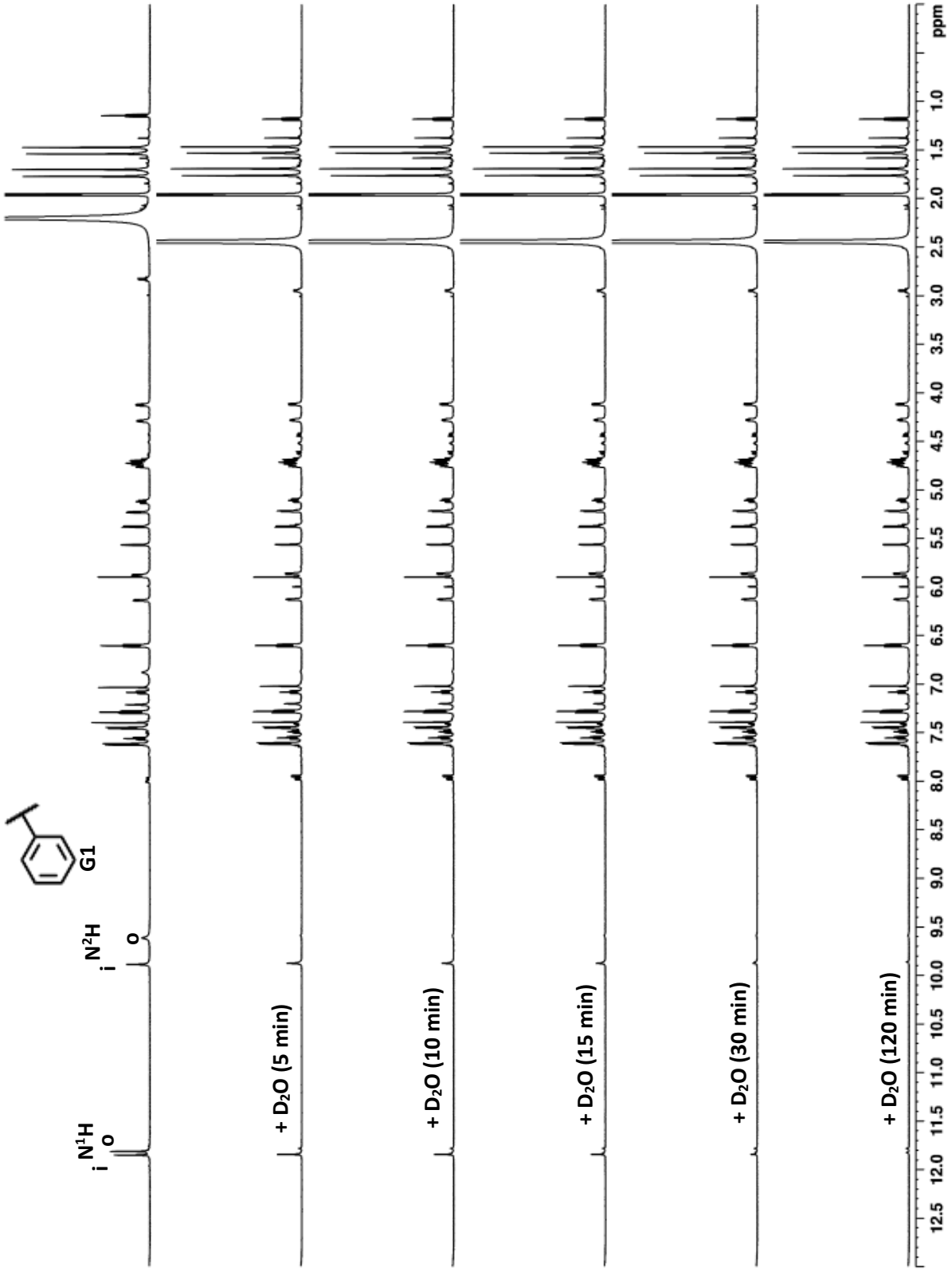

Figure S25**.** Entire spectra for the H/D exchange of amide N^1H and amino N^2H protons of [**G1**]$_{16}$•3K$^+$3I$^-$ (0.625 mM) in CD_3CN after addition of 10 μL D_2O.

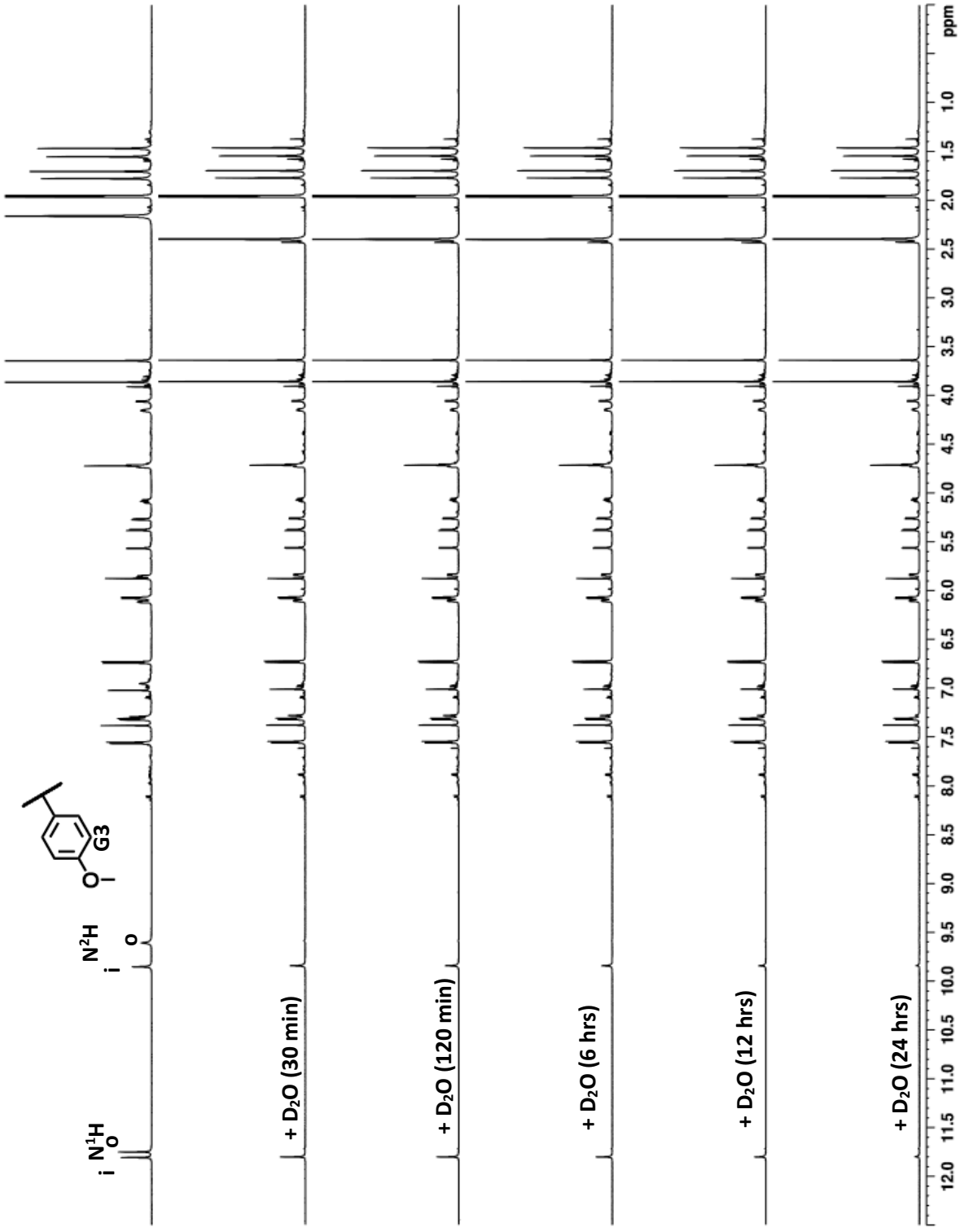

Figure S26**.** Entire spectra for the H/D exchange of amide N^1H and amino N^2H protons of [**G3**]$_{16}$•3K$^+$3I$^-$ (0.625 mM) in CD_3CN after addition of 10 μL D_2O.

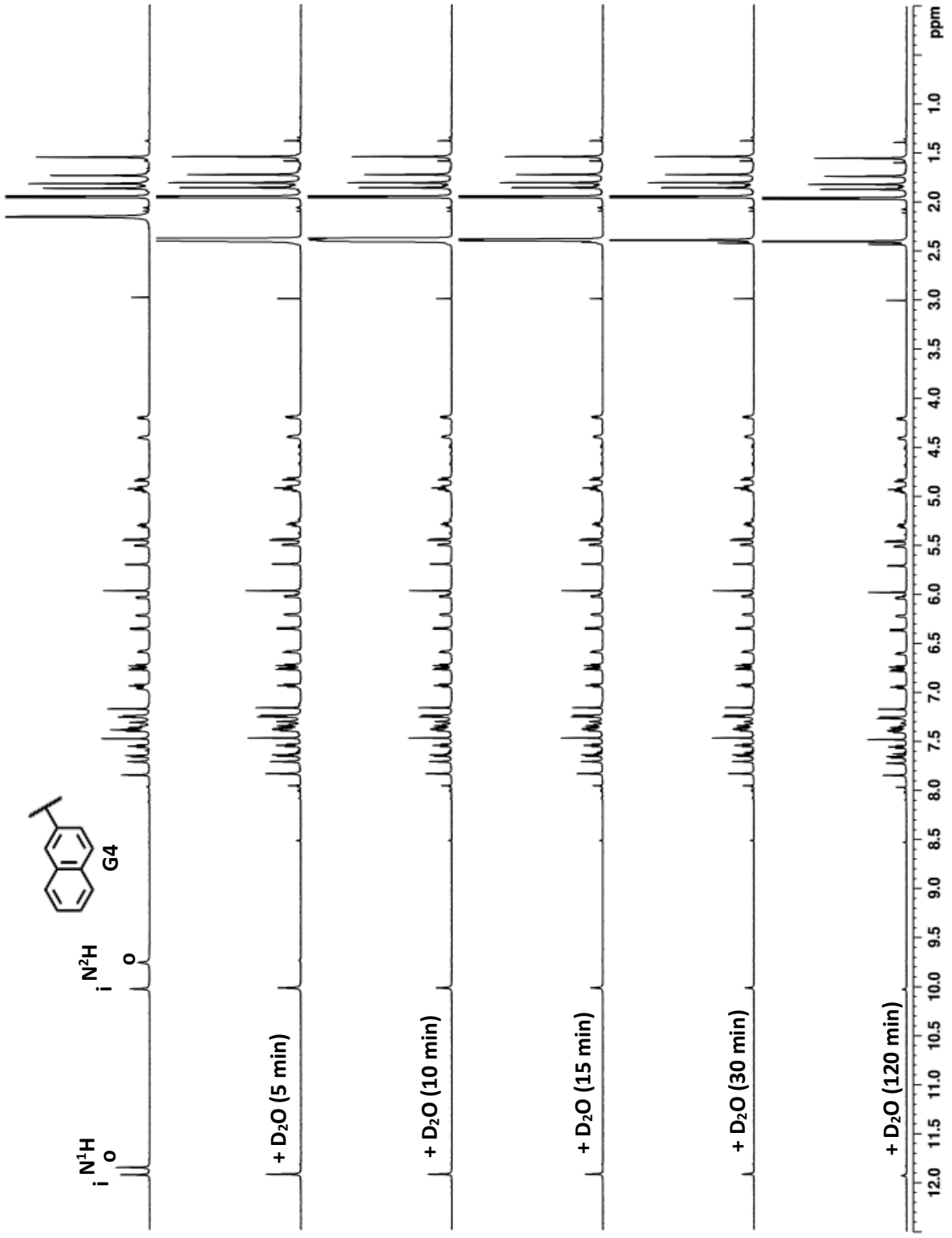

Figure S27**.** Entire spectra for the H/D exchange of amide N^1H and amino N^2H protons of [**G4**]$_{16}$•3K^+3I^- (0.625 mM) in CD_3CN after addition of 10 μL D_2O.

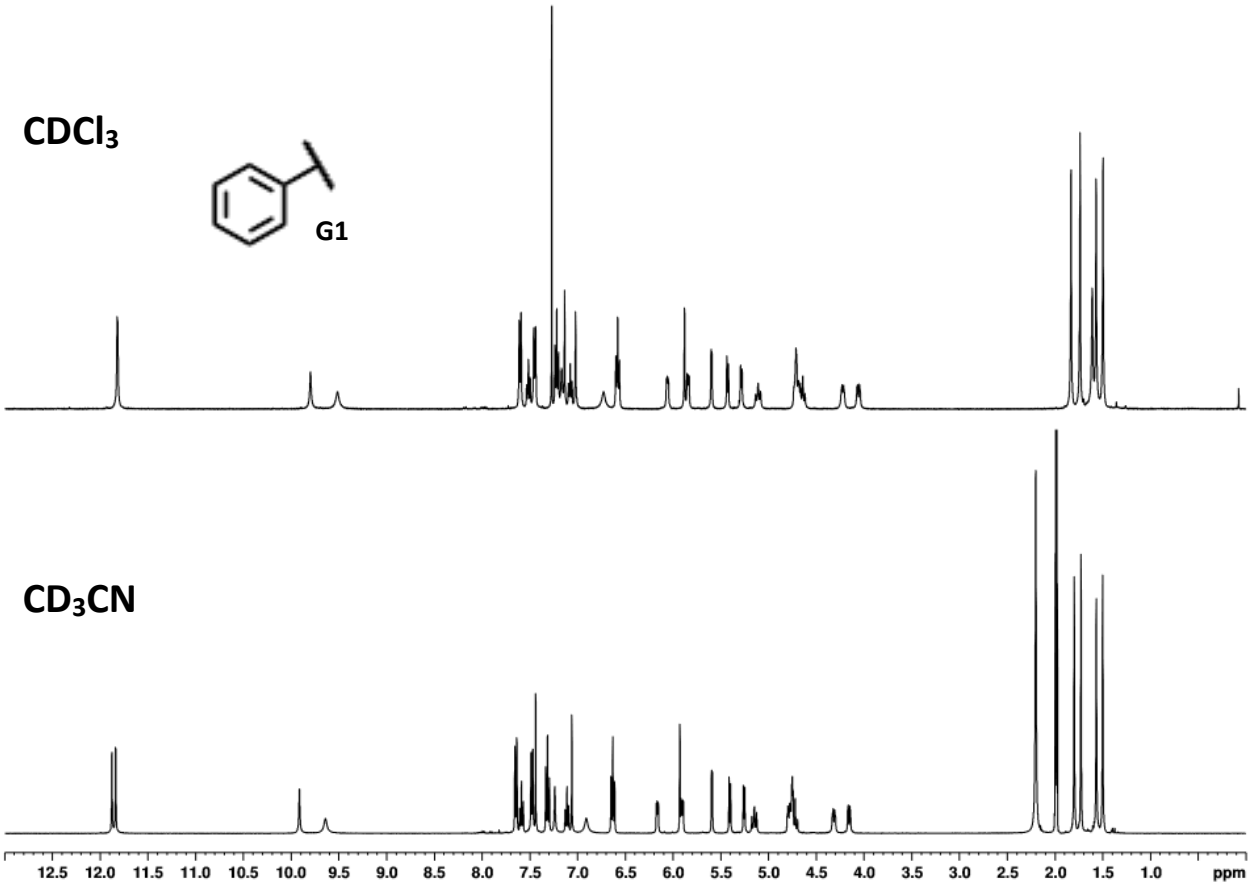

Figure S28. Comparative ^{1}H NMR spectra of $[\mathbf{G1}]_{16}\bullet 3K^{+}\ 3I^{-}$ in $CDCl_3$ and CD_3CN.

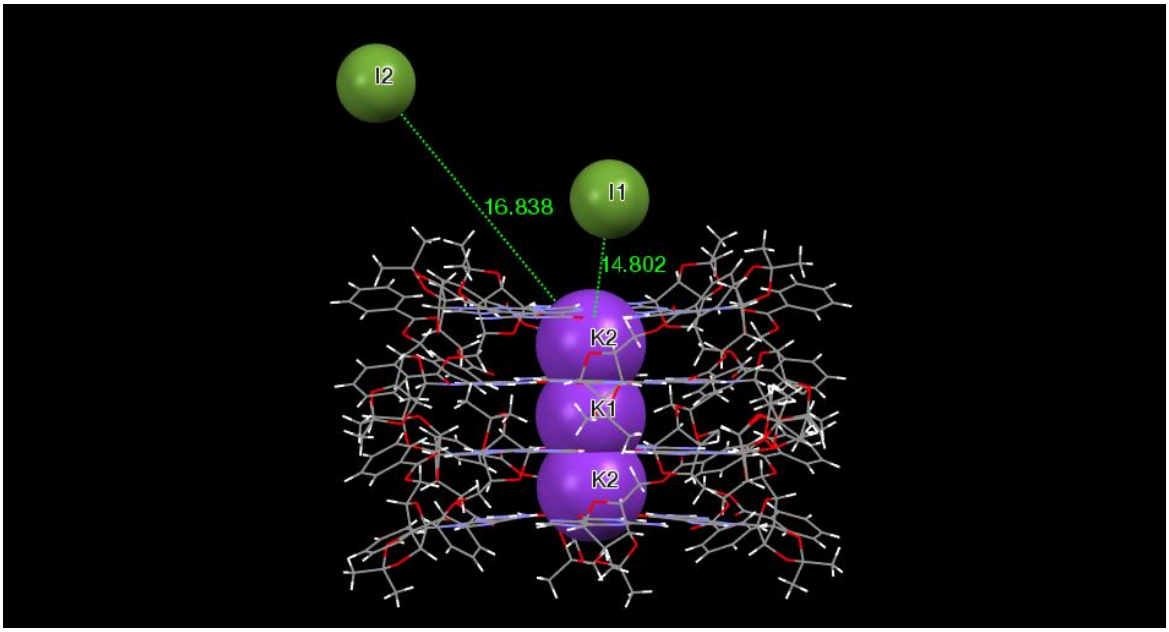

Figure S29. Depiction of X-ray crystal structure of $[\mathbf{G1}]_{16} \bullet 3K^{+}\ 3I^{-}$. The K+ atoms are depicted as purple spheres and the iodide anions are depicted as green spheres. Distances between K2 and the 2 unique iodide anions (I1 and I2) are 14.802 and 16.838 angstroms, respectively . This figure shows that the iodide anions do not interact with the hexadecamer $[\mathbf{G1}]_{16} \bullet 3K^{+}\ 3I^{-}$.

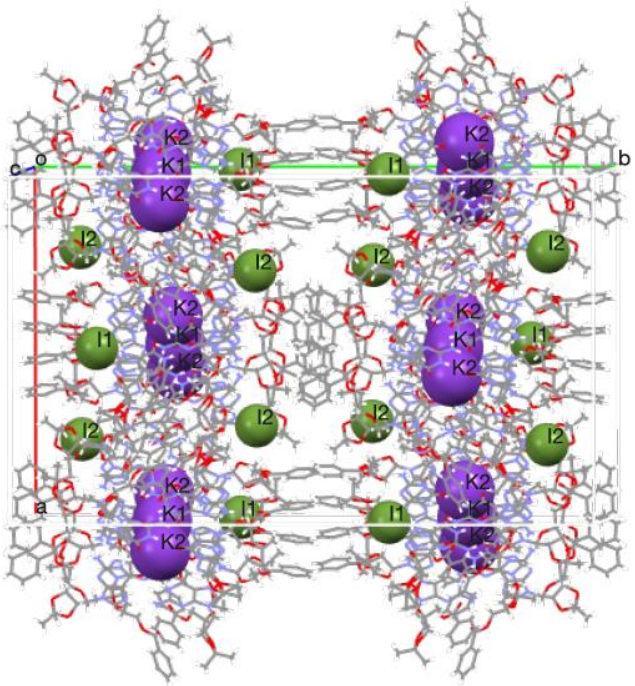

Figure S30. Depiction of the unit cell for $[\mathbf{G1}]_{16} \bullet 3K^{+}\ 3I^{-}$. The K+ atoms are depicted as purple spheres and the iodide anions are depicted as green spheres. More details can be found by accessing structure # CCDC-1495606 at the Cambridge Crystallographic Data Centre.